Global Challenges
www.global-challenges.com

A Solar to Chemical Strategy: Green Hydrogen as a Means, Not an End

Gabriel A. A. Diab, Marcos A. R. da Silva, Guilherme F. S. R. Rocha, Luis F. G. Noleto, Andrea Rogolino, João P. de Mesquita, Pablo Jiménez-Calvo, and Ivo F. Teixeira**

Green hydrogen is the key to the chemical industry achieving net zero emissions. The chemical industry is responsible for almost 2% of all CO_2 emissions, with half of it coming from the production of simple commodity chemicals, such as NH_3, H_2O_2, methanol, and aniline. Despite electrolysis driven by renewable power sources emerging as the most promising way to supply all the green hydrogen required in the production chain of these chemicals, in this review, it is worth noting that the photocatalytic route may be underestimated and can hold a bright future for this topic. In fact, the production of H_2 by photocatalysis still faces important challenges in terms of activity, engineering, and economic feasibility. However, photocatalytic systems can be tailored to directly convert sunlight and water (or other renewable proton sources) directly into chemicals, enabling a solar-to-chemical strategy. Here, a series of recent examples are presented, demonstrating that photocatalysis can be successfully employed to produce the most important commodity chemicals, especially on NH_3, H_2O_2, and chemicals produced by reduction reactions. The replacement of fossil-derived H_2 in the synthesis of these chemicals can be disruptive, essentially safeguarding the transition of the chemical industry to a low-carbon economy.

1. Introduction

In today's world, addressing the challenges associated with energy production has become vital. Fossil fuel dependence, climate change concerns, geopolitical wars, and the need for sustainable alternatives have propelled the exploration of innovative solutions. Among renewable energies such as wind and hydropower, solar energy stands out as a promising and suitable solution due to the abundant amount of energy available from solar.[1]

1.1. Solar Energy and Low-Carbon Economy

The abundant and renewable power of the sun provides a direct irradiated energy of 3.8×10^{24} J per year.[2] Considering the global energy demand was $82{,}2 \times 10^{18}$ J in 2019, this means that capturing a small portion of the sun's energy could supply such global demand.[3] Therefore, solar energy conversion into chemicals offers a way to convert solar photons into storable and transportable fuels or valuable chemicals.[4] Nevertheless, the effective capture of solar photons encompasses geographic location, daylight availability, and seasonal variations.[5] Solar energy chemical conversion holds the potential to mitigate greenhouse gas emissions, reduce reliance on fossil fuels, and pave the way toward a cleaner and more sustainable energy future.

G. A. A. Diab, M. A. R. da Silva, G. F. S. R. Rocha, L. F. G. Noleto, J. P. de Mesquita, I. F. Teixeira
Department of Chemistry
Federal University of São Carlos
Rod. Washington Luís km 235 – SP, São Carlos, SP 13565-905, Brazil
E-mail: ivo@ufscar.br

A. Rogolino
Cavendish Laboratory
University of Cambridge
Cambridge CB3 0HE, UK

J. P. de Mesquita
Departamento de Química
Universidade Federal dos Vales Jequitinhonha e Mucuri
Rodovia MGT 367 – Km 583, n° 5000, Alto da Jacuba, Diamantina, MG 39100, Brazil

P. Jiménez-Calvo
Department for Materials Sciences
Friedrich-Alexander-Universität Erlangen-Nürnberg
Martensstrasse 7, D-91058 Erlangen, Germany
E-mail: pablo.jimenez.calvo@mpikg.mpg.de

P. Jiménez-Calvo
Chemistry of Thin Film Materials
Friedrich-Alexander-Universität Erlangen-Nürnberg
IZNF, Cauerstraße 3, D-91058 Erlangen, Germany

The ORCID identification number(s) for the author(s) of this article can be found under https://doi.org/10.1002/gch2.202300185

© 2023 The Authors. Global Challenges published by Wiley-VCH GmbH. This is an open access article under the terms of the Creative Commons Attribution License, which permits use, distribution and reproduction in any medium, provided the original work is properly cited.

DOI: 10.1002/gch2.202300185

A low-carbon economy, in conjunction with a circular sustainable economic system, establishes a series of collective measures, following the Paris Agreement,[6] Roadmap and Net Zero by 2050,[7] and the Latin American Deep Decarbonization Pathways project.[8] One of these measures involves the adoption of energy-efficient processes, especially for hydrogen (H_2) production, since is a multifunctional molecule for a wide range of applications, being a key driver for sustainability.[9]

1.2. Hydrogen: Energy Vector and Production

H_2 has emerged as a crucial element in the pursuit of carbon neutrality. With its versatile applications and potential for zero-emission energy generation, H_2 has the capacity to play a key role in achieving carbon neutrality and advancing the transition to renewables.[10]

The importance of H_2 as an energy carrier relies upon its high energy density per mass. However, transport considerations need to be taken considering its volumetric density. Regardless of its state (liquid or gas), the energy density of H_2 per mass is 128 MJ kg^{-1}, surpassing the energetic content of conventional fossil fuels such as natural gas, gasoline, propane, and methane by nearly twofold. When compared to ethanol and coal, H_2 boasts an impressive energy content that is 7 to 8 orders of magnitude higher. However, the volumetric density of H_2 varies depending on its chemical state. Liquid H_2 has a density of 71 Kg m^{-3} at −253 °C and 1 bar, while compressed H_2 gas density is 42 Kg m^{-3} at ambient temperature and 700 bar. In this context, the compression step is vital for practical H_2 transport, as it allows for higher gas energy carrier quantities in a standard 25 L gas container compared to liquid H_2. The compression of H_2 gas varies depending on the applied pressure, ranging from 200 to 700 bar. As a result, the volume unit can accommodate either less or more H_2 gas content. However, this increased transportability comes at an extra cost due to the added compression step.[9,11]

Worldwide H_2 production currently stands at 90 million metric tons, and it is projected to exceed 200 and 500 million metric tons in 2030 and 2050, respectively.[12,13] Yet, the majority of production processes rely on fossil fuels (98%), resulting in 900 million metric tons of CO_2 emissions annually.[12] The rising demand is primarily met through energy-intensive and polluting methods like steam methane reforming (76%) and gasification (22%). In contrast, electrolysis accounts for a minor share of 4%.[13,14] Efforts to shift toward cleaner and emerging production methods are needed.

With regard to the process of obtaining and the environmental impact of the production technology, hydrogen is classified as grey, blue, turquoise, white, and green. This ranking ranges from the most environmentally harmful to the most climate-friendly hydrogen production technologies, including the natural origin.[14] Grey hydrogen is currently the most common way to obtain hydrogen. In this process, hydrogen is obtained from steam methane reformation using natural gas and/or methane as precursors. In the reaction, the methane is subjected to high-temperature and pressure in the presence of steam (H_2O) and a Ni-based catalyst to produce H_2 and CO_2. In addition to the use of non-renewable fuel, the process consumes a lot of energy and emits thousands of tons of CO_2 into the atmosphere. Blue hydrogen is obtained in a similar way to grey hydrogen. However, the greenhouse gases generated are captured and stored, reducing the environmental impact. Although it is estimated that total carbon dioxide equivalent emissions for blue hydrogen are ≈10% lower than for grey hydrogen, which mischaracterizes the technology as being low carbon.[15] Turquoise hydrogen is obtained from a different chemical route, the pyrolysis of methane.[16] In this process, hydrogen gas and solid carbon are obtained as products. Although not yet used at scale, the strategy can be a less harmful alternative if the thermal process is electrified, using renewable energy sources. White hydrogen is naturally produced deep inside the Earth's crust through a geochemical process. It is a cost-effective and carbon-neutral method, comparable to fossil fuels. The production process resembles that of natural gas, including prospecting, site selection, drilling, extraction, and product separation. Environmental protection is of paramount importance in implementing this solution.[17] Finally, hydrogen considered "green" is obtained from water splitting using sustainably sustainable sources, such as electricity generated from wind and solar or photocatalysis powered by sunlight.[17] Although electrolysis fed by renewable power sources is emerging as the most promising strategy, photocatalysis presents advantages that might be underestimated and could hold a bright future for this topic.

The photocatalytic approach can be considered the cleanest, direct, and sustainable method for hydrogen production.[18] By mimicking natural photosynthesis, this process utilizes water as its sole substrate. However, unlike the natural counterpart, artificial photocatalysis requires a versatile catalyst and an energy input to initiate the charge transfer and drive the two half-reactions that effectively split water into oxygen and H_2 (**Figure 1**).[19]

$$H_2O + 2h^+ \rightarrow \frac{1}{2}O_2 + 2H^+ \quad (1)$$

$$2H^+ + 2e^- \rightarrow H_2 \quad (2)$$

1.3. H_2 Applications in the Chemical Industry

The hydrogen technological roadmap within the chemical industry is quite extensive. Around 90% of the hydrogen produced is consumed in oil refining (hydrocracking, desulfurization) (≈42%), ammonia (≈35%), methanol (≈15%) production, and the remaining ≈8% in other chemicals, such as H_2O_2 production and steel manufacturing (direct reduced iron – DRI).[20] In 2021, the global demand for hydrogen increased by 5% compared to 2019 (pre-pandemic), driven mainly by the production of chemicals.[21]

Currently, ≈70% of the ammonia produced (the main chemical produced from hydrogen) is converted into fertilizer (NPK, urea, and ammonium nitrate) and only 3% of the ammonia is used directly (Ammonia Technology Roadmap). The remainder of global ammonia demand is for a range of industrial applications. Among the main chemical compounds produced from ammonia are pharmaceutical products, amines, acrylonitrile, and nitric acid, which are used, among other applications, in the production of explosives and polymeric materials. Although the main use of urea, a direct derivative of ammonia, obtained from the reaction with carbon dioxide, is as nitrogenous fertilizer,

 © 2023 The Authors. Global Challenges published by Wiley-VCH GmbH

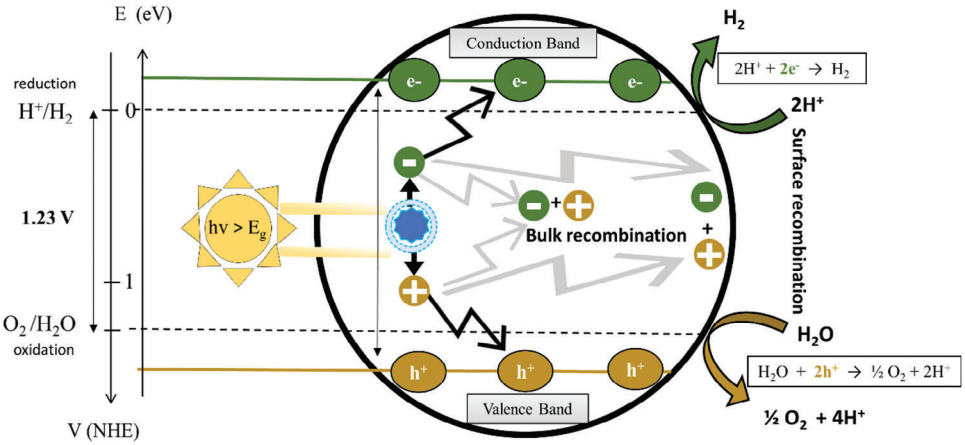


Figure 1. Scheme illustrating the water splitting reaction using a semiconductor-based photocatalyst. Reproduced with permission.[9] Copyright 2023, Elsevier.

≈20% of the production is used in different industrial applications, the main one being in the manufacture of resins, especially those based on in urea-formaldehyde.[21] Acrylonitrile is another important derivative of ammonia, obtained from the reaction between propylene, ammonia, and oxygen. Additionally, it is a chemical intermediate for the production of various polymeric materials, including polyacrylonitrile, polyurethanes, and nylons.[22]

Other hydrogen direct derivatives with significant industrial importance are aniline and hydrogen peroxide. Their direct use and derivatives have major impacts on different industrial sectors, including durable chemical products, paper and cellulose, pharmaceuticals, food, textiles, and others.[23] Aniline is obtained from the hydrogenation of nitrobenzene, which is obtained through the reaction of benzene in concentrated nitric acid.[24] It is estimated that ≈10 million tons are produced per year for use in the production of polyurethanes from diphenyl methane, 4′-diisocyanate derivative, rubber additives, and a wide variety of chemical compounds, including pesticides, dyes, and pharmaceuticals.[25]

Currently, more than 6.5 million metric tons of hydrogen peroxide are produced worldwide, with more than 90% being produced through the anthraquinone AO process, in which hydrogen and oxygen react in the presence of anthraquinone.[26] The main demands of hydrogen peroxide are in the pulp and paper industries, as bleaching agents in textiles, liquid and solid detergents, water treatment, semiconductor cleaning, and propylene oxide production.[27] In light of the pivotal position role of hydrogen in the chemical industry, developing routes to obtain commodity chemicals, such as ammonia, aniline, and hydrogen peroxide, without relying on fossil-derived hydrogen is of paramount importance to enable a transition to a sustainable and CO_2-free chemical industry.

1.4. Advantages of H_2 Direct Use

Photocatalysis as well as electrolysis can provide a route to green hydrogen production. However, the photocatalysis approach holds much greater potential; it can be employed as a strategy to directly convert the hydrogen generated from water into chemicals. The direct utilization of H_2 for chemical production offers environmental, renewable energy, versatility, energy efficiency, and sustainability advantages, making it an attractive option for the chemical industry.[28]

In this direction, using H_2 directly to produce chemicals offers several advantages:

(a) Environmental Benefits: Chemical production can significantly reduce carbon emissions compared to conventional methods. By avoiding intermediate steps or fossil fuel inputs, the process can help mitigate greenhouse gas emissions and contribute to a more sustainable and low-carbon economy.

(b) Renewable and Clean Energy Source: Utilizing this direct conversion of green H_2 for chemical strategy leads to greener and more sustainable processes, where ideally all the energy input will come from sunlight.

(c) Versatile Feedstock: As mentioned, H_2 is a platform molecule in the chemical industry, participating in various reactions enabling the production of a wide range of chemicals. Its versatility allows for the synthesis of different compounds and can serve as a valuable building block in various industrial processes.

(d) Energy Efficiency: Green H_2 generated by photocatalysis often exhibits high selectivity and can operate under milder conditions, reducing energy requirements compared to traditional processes. With efficiency gains, this might translate into cost savings and reduced resource consumption in the future.

(e) Reduced Dependency on Fossil Fuels: By utilizing green H_2 directly, the reliance on fossil fuel feedstocks can be minimized. This reduces vulnerability to fossil fuel price fluctuations and supply disruptions, creating a more stable and sustainable chemical industry. In other words, the chemical industry relies mainly on the widely available sunlight and not on fossil fuels.

(f) Potential for Circular Economy: The H_2 generated by photocatalysis can be helped by sacrificial reagents, which can

 © 2023 The Authors. Global Challenges published by Wiley-VCH GmbH

be chosen according to the principles of a circular economy. It enables the conversion of waste or by-products into hydrogen sources and ultimately into valuable chemicals. This approach promotes resource efficiency and waste reduction, contributing to a more circular and sustainable industrial ecosystem.

Therefore, integrating the production of H_2 and chemical conversion processes within the same site offers significant advantages. By eliminating the need for separate storage facilities, a continuous process can be achieved, allowing ultimately energy storage into chemicals. This strategy solves one of the greatest challenges in the hydrogen economy, which is H_2 storage. This integration has the potential to optimize resource utilization, reduce costs, and enhance the overall efficiency of the hydrogen-based chemical production system.

2. Photocatalytic-driven Ammonia Production

Currently, there is great interest from the scientific community worldwide in developing technological alternatives for the synthesis of ammonia (or atmospheric nitrogen fixation) to replace the Haber-Bosch process, which is widely regarded as costly from both environmental and energy standpoints.[29]

Ammonia is the second most produced chemical in the world, with an estimated production of ≈200 million tons per year.[30] However, its significance extends beyond sheer production volume, as it is considered one of the most crucial chemicals due to its immense demand in food production (primarily as fertilizers) and its widespread usage in the chemical industry. Furthermore, ammonia has the potential to play a central role as a hydrogen storage strategy within the future hydrogen economy. Regarding hydrogen storage, in addition to an H_2 content of 17.65%, NH_3 has been recommended as the most technically viable option because of its properties that allow liquefaction under milder temperature and pressure conditions. Additionally, it offers greater safety for storage and transport due to its low vapor pressure and higher boiling point.[31]

Worldwide ammonia production is dominated by the Haber–Bosch process. In this process, gaseous nitrogen (N_2) and gaseous hydrogen (H_2) react at elevated temperature (400-°C) and pressure (10–15 MPa), over an iron (Fe)-based catalyst. In addition to the extreme reaction conditions, the process consumes ≈1-% of the world's energy production[32] and contributes 1.2% of the total global CO_2 emission, as hydrogen gas is obtained using non-renewable feedstock, specifically steam methane reforming ($CH_4 + 2H_2O \rightarrow 4H_2 + CO_2$) or coal gasification ($C + 2H_2O \rightarrow 2H_2 + CO_2$). Despite the high energy and environmental cost, the use of the Haber-Bosch process within the context of an economy based on the use of fossil fuels had a positive impact on the economy and food production.[33] However, in the process of global decarbonization, it is urgent to change the ammonia production process as a way to drastically reduce both CO_2 emissions and high energy consumption. As it was at the beginning of the last century, ammonia synthesis is considered a great and fascinating challenge of the 21st century, playing a key role in a sustainable future.[34]

The electrification of the Haber-Bosch process is a more realistic alternative at first, as it replaces the use of fossil sources by electrolysis of water to supply hydrogen.[35] On the other hand, the intrinsic high-energy demand of the process remains. Evidently, the use of alternative sources of energy generation can justify this strategy, but from a future perspective, the industrial process will need significant changes for the desired energy revolution to be achieved. This realization will only happen by exploring green, sustainable, mild, and economic nitrogen fixation strategies.[36]

In this context, the nitrogen fix employs a catalyst directly photoactivated by sunlight to promote the reduction of atmospheric N_2 into NH_3, in which water or other sustainable proton source is the source of protons, under ambient conditions. This is the strategy that holds the greatest potential for enabling green and sustainable ammonia production since it ideally does not require the production of hydrogen gas and the use of high temperature and pressure (**Figure 2**).

In the Haber-Bosch process, molecular bonds are broken to form nitrogen and hydrogen atoms through a dissociative mechanism,[37] as adding the first hydrogen atom is challenging (Equation 3).[38] In nitrogen fixation using photocatalysis, molecular nitrogen adsorbed on the catalyst surface is reduced in the conduction band by excited electrons from the valence band (Equation 4), and the electronic structure is restored through the oxidation of water into molecular oxygen (Equation 5). This oxidation provides the protons for the formation of NH_3.[39] This uphill reaction requires a potential greater than 1.14 eV.

$$N_{2(g)} + H^+_{(aq)} + e^- \rightarrow N_2H_{(ads)} (-3.2 \text{ V vs RHE}) \quad (3)$$

$$N_{2(g)} + 6H^+_{(aq)} + 6e^- \rightarrow 2NH_{3(g)} (0.092 \text{ V vs SHE}) \quad (4)$$

$$H_2O_{(l)} \rightarrow \frac{1}{2}O_{2(g)} + 2H^+_{(aq)} + 2e^- (1.23 \text{ V vs SHE}) \quad (5)$$

The first demonstration of nitrogen fixation through photocatalysis was reported in 1977 by Schrauzer and Guth.[40] Subsequently, Schrauzer et al. showed that N_2 photofixation occurs on finely dispersed titanium minerals, such as rutile, present on sand surfaces from different geographic locations.[41] From this pioneering demonstrative studies on the possibility of producing ammonia on the surface of a catalyst using light have given rise to a new research sector within photocatalysis, which has seen significant growth in the last decade and even greater interest from researchers in recent years. The growing interest is evident from the results generated by the ISI Web of Science database using "nitrogen fixation photocatalysis", "ammonia photocatalysis" or "nitrogen photoreduction nitrogen fixation". Between 2002 and 2012, 293 studies were reported. From 2013 to 2023, out of 1317 works, 793 were published from 2020 onward, demonstrating extensive recent research interest.

To facilitate the discussion of the main challenges associated with the application of photocatalysis for the production of ammonia, it is necessary to understand the basic mechanism of photocatalysis. First, we will consider that the photocatalyst has efficient photon absorption and the valence and conduction bands are ideally positioned for the oxidation and reduction of the target molecules, in this case N_2 and an electron donor, such as water or another sacrificial agent. After the absorption of photons with energy equivalent to the band gap of the semiconductor, the elec-

 © 2023 The Authors. Global Challenges published by Wiley-VCH GmbH

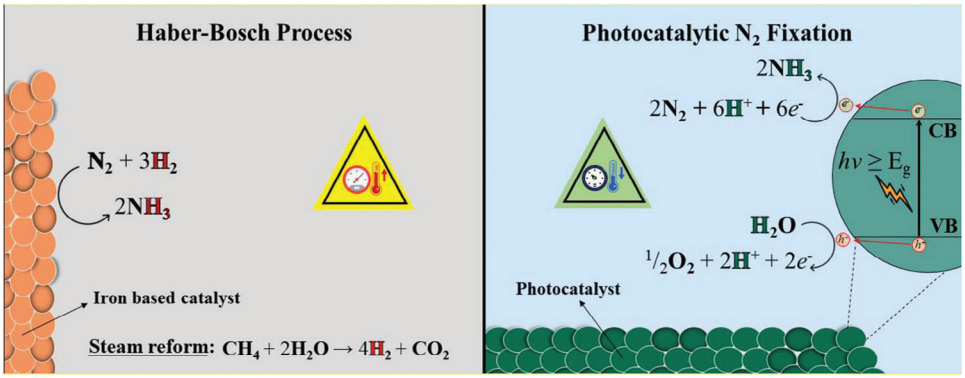


Figure 2. Comparative scheme representing the ammonia production from the traditional Haber-Bosch process and the photocatalytic approach where water is the electron donor.

tron donor is oxidized in the valence band, while N_2 molecules are adsorbed on the surface and reduced in the conduction band by the photoexcited electrons. **Figure 3** shows the redox potentials of the reduction of the N_2 molecule (1 electron) on the surface of a photoactivated semiconductor.

Currently, solar-driven nitrogen fixation faces several main challenges, including the inhibition of h^+/e^- recombination, N_2 chemisorption, and activation.[43] As a consequence, the production rates for most studied photocatalysts remain significantly lower than desired, making the success of the solar fixation of N_2 still distant.[39] In fact, the vast majority of results show production on the order of μmol h^{-1} g^{-1}.[44] Despite the photocatalytic ammonia production using water as an electron donor being the most attractive and sustainable condition, the kinetics of the process represents a challenge due to the complexity involving the multi-electron oxidation of H_2O, which is inhibited by the rapid recombination rate of photogenerated electron-hole pairs. Introducing sacrificial agents of renewable origins, such as methanol, glycerol, or even wastewater,[45] and biomass[46] could improve charge separation and consequently the overall quantum efficiency of the reaction, as sacrificial electron donors supply the holes in the semiconductor the presence of sacrificial agents may also inhibit the oxidation of the ammonia produced,[47] capturing eventual oxidizing radicals formed in parallel reactions. A more interesting alternative to the use of sacrificial agents lies in coupling the ammonia photofixation with the conversion of sacrificial agents through selective oxidation to value-added chemicals.[48]

To date, TiO_2 is one of the most investigated photocatalysts for this reaction due to its superior photoactivity, but its high band gap (≈3.2 eV) and poor utilization of the solar spectrum have motivated the application and development of new materials. This has led to several modification strategies over recent years, such as noble metal deposition (co-catalysis),[49] defect engineering,[50]

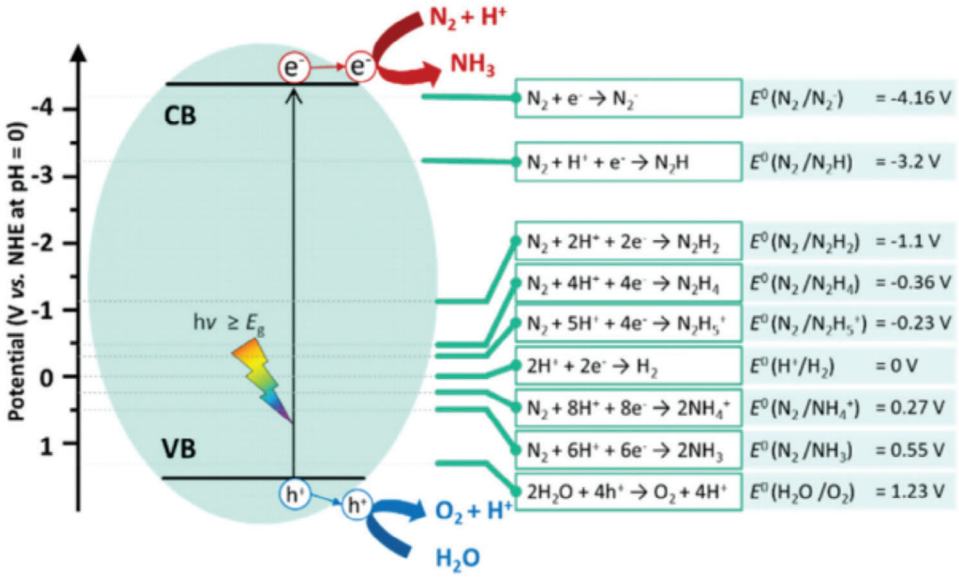


Figure 3. Schematic representation of photocatalytic N_2 reduction on a photoactivated semiconductor and the respective redox potentials associated with the reduction of N_2 from 1 to 6 electrons. For comparison purposes, the redox potentials of the water are also shown. Reproduced with permission.[42] Copyright 2021, Royal Society of Chemistry.

 © 2023 The Authors. Global Challenges published by Wiley-VCH GmbH

Table 1. Summary of different photocatalysts applied for N_2 fixation.

Catalyst	Hole scavenger employed	Catalyst mass [mg]	Light wavelength [nm	NH_3 rate [μmol g^{-1} h^{-1}]	AQY [%]	Reference
Ti_3C_2-TiO_2	CH_3OH (20%)	50	420	415.6	N/A	[51]
NTO.5	H_2O	N/A	350–780	80.09	0.07 (375 nm)	[52]
Sb/TiO_2	MeOH (20%)	N/A	>420	20.82	N/A	[53]
BOB-OV	H_2O	50	420–780	104.2	0.23 (420 nm)[a]	[60]
Bi_5O_7Br0	H_2O	25	400	12 720	N/A	[61]
Ru-CCN.05	H_2O	50	Xenon lamp	132,69	N/A	[58]
Cu-CN	EtOH (20%)	50	420	186	N/A	[65]
Fe-T-S	H_2O	50	Xenon lamp	32	N/A	[66]

[a] External quantum efficiency (EQE).

doping, and surface tailoring. For example, Ding et al. found that N-doping in Ti_3C_2-TiO_2 improved the ammonia production yield to 415.6 μmol h^{-1} g^{-1} (8 times that of pure TiO_2) due to the enhanced charge separation facilitated by the doping.[51] Li et al. also demonstrated an increase from 31.50 to 80 μmol h^{-1} g^{-1} using N-doping in TiO_2.[52] This strategy often generates defects and oxygen vacancies that promote better adsorption and activation of N_2, as well as increased separation and migration of photogenerated carriers. TiO_2 loaded with Sr (Sr/TiO_2) also exhibited efficient separation and migration of photogenerated charges. This catalyst yielded an NH_3 rate of 32.2 μmol h^{-1} g^{-1} (547.4 mg h^{-1} g^{-1}) under full spectrum light and 20.8 μmol h^{-1} g^{-1} (353.9 mg h^{-1} g^{-1}) under visible light illumination, surpassing Sb nanosheets and pure a-TiO_2 by factors of 2 and 16, respectively.[53]

Various materials have been considered for photocatalytic nitrogen fixation (**Table 1**), such as metal oxides, metal sulfides, layered double hydroxides, and carbon-based materials including carbon nitride,[54,55] bismuth-based materials,[56] single atom catalysis,[55,57,58] and metal-organic frameworks (MOFs).[59] Among these materials, the most promising results for photocatalytic nitrogen fixation have been observed for bismuth-based materials. In 2015, Li et al. reported one of the first studies on catalysts based on bismuth oxyhalides.[60] The authors prepared an active catalyst in the visible region absorption based on BiOBr nanosheets containing oxygen vacancies on the exposed 001 facets. The visible-light-driven photocatalytic N_2 fixation rate was estimated to be 104.2 μmol h^{-1} g^{-1} when using water as a proton donor, without the need for precious-metal cocatalysts. More recently, Li et al. presented Bi_5O_7Br as a photocatalyst with well-defined nanotube structures under visible-light irradiation, achieving an impressive rate of 12.72 mM g^{-1} h^{-1} for nitrogen fixation.[61]

Unlike heterogeneous catalysts, single-atom catalysts (SACs) in general offer the high efficiency and selectivity presented by homogeneous catalysts, but with the robustness and manipulation advantages associated with heterogeneous catalysis.[62] SACs represent the new frontier in the development of photocatalysts,[63] bringing several important concepts. Apart from their high atomic efficiency, SACs possess a unique electronic structure and adjustable coordination environments for the active sites,[64] which have been successfully exploited in the photocatalytic nitrogen fixation reaction. Li et al. prepared a single-atom ruthenium catalyst on the surface of the graphitic carbon nitride (g-C_3N_4). They obtained a material with 5% ruthenium and significant structural defects (cyano groups) on the surface of the support, which was then for nitrogen fixation using only water as a proton source. The catalytic performance of the material containing single atom sites was better than that observed for bare g-C_3N_4 by 1,5 times. The rate of photocatalytic nitrogen fixation obtained in ultra-pure water was 132 μmol g^{-1} h^{-1}.[58]

Xie et al. reported a single Cu atom supported on porous g-C_3N_4. The authors demonstrated that Cu single atoms were immobilized at the defect sites of g-C_3N_4 via the formation of Cu-N bonds. By integrating nitrogen adsorption sites and the electron accumulation on the Cu single atom, the catalytic activity of SAC was nine times higher than that observed for pristine g-C_3N_4, achieving an ammonia yield of 186 μmol g^{-1} h^{-1}.[65] Similarly, Fe single atom immobilized on mesoporous TiO_2-SiO_2 displayed an ammonia generation rate of 32 μmol g^{-1} h^{-} without any sacrificial agent. Experimental and theoretical calculations confirmed the formation of photoinduced high-valent Fe(IV) species, which played a dual role in water oxidation and N_2 hydrogenation, primarily at neighboring oxygen vacancies.[66]

In fact, overcoming the inhibition of recombination and increasing exciton lifetime are crucial challenges for photocatalysis in sustainable ammonia synthesis. Developing heterojunctions represents an interesting and rational strategy to address these issues.[34] Although some works show positive results, type I heterostructures generally yield lower results compared to type II heterojunctions. This difference arises because, in type I heterostructures, electrons and holes are concentrated within the same semiconductor, theoretically facilitating recombination. In contrast, in type II heterostructures, while the holes are concentrated on semiconductor A, the excited electrons are concentrated on semiconductor B. This spatial separation delays recombination, increasing the likelihood of electron transfer reaction on the photocatalyst's surface.

Defect engineering, cocatalysis, and heterojunctions strategies have indeed led to improvements in the activity, but they have generally fallen short of meeting established objectives. Nevertheless, there has been a significant surge in interest in this field over the past 5 years, which is expected to yield more promising results in a relatively short period. Many of the primary challenges have already been identified and addressed.[67] Due to the

 © 2023 The Authors. Global Challenges published by Wiley-VCH GmbH

slow oxidation rate of water as a proton supplier for nitrogen reduction, the use of sacrificial agents appears to be inevitable. In this context, the coupling of an ammonia production system with industrial waste treatment or the synthesis of valuable by-products should be considered an intriguing strategy for the feasibility of photocatalytic nitrogen fixation. However, the development of these coupled systems presents challenges similar in magnitude to ammonia photofixation itself. This requires the development of specific catalysts with unique structural and electronic characteristics for each photoreactor, underscoring the pivotal role of photoreactor design in this process.

3. Photocatalytic-driven Hydrogen Peroxide Production

Hydrogen peroxide is one of the simplest molecules in nature with enormous relevance to industry. Its varied applications ranging from the biomedical industry to cosmetics, establish it as one of the most versatile light chemicals. It plays an essential role in the paper industry as a bleaching agent for cellulose,[68] it is a powerful bactericidal agent extensively used in water treatment,[69] where it also contributes to the degradation of organic pollutants.[70] More importantly, because of its chemical reactivity, it can be considered a green oxidant, only releasing water and oxygen as by-products, which is highly relevant to the pharmaceutical industry.[27] Hydrogen peroxide also finds a useful generator of reactive oxygen species (ROS) in the iron-catalyzed Fenton reaction.[71] Lastly, it is a promising substrate for fuel cells, where it can play a dual role, contributing to current generation at both the cathode and the anode, enabling electricity generation from a single chemical source.[72] The global market value of hydrogen peroxide was estimated to be ≈3.2 billion US dollars in 2022 and is expected to increase to 4.0 billion in the next five years.[73]

Hydrogen peroxide is a valuable chemical that can be synthesized from the second most abundant gas in our atmosphere (i.e., O_2). Three main synthetic routes can be identified: i) redox neutral comproportionation of H_2 and O_2, ii) reductive oxygen reduction reaction (ORR) reaction, and iii) oxidative water oxidation reaction (WOR). Although an excellent example of atom economy,[74] it is evident that the first method must rely on green hydrogen for sustainable implementation. Nevertheless, hydrogen/oxygen mixtures pose risks of explosion, as well as engineering challenges related to gas storage and delivery.[75] Therefore, redox conversion from abundant O_2 or H_2O is the preferred strategy for sustainable H_2O_2 synthesis. Such chemical reactions easily occur at mild conditions in the regime of electrocatalysis, where electricity can be generated from wind turbines, photovoltaic cells, or through photocatalysis. The latter is usually fulfilled by means of light-absorbing semiconductors, that in turn, transfer excited electrons or holes to adsorbed substrates. Catalyst design for direct solar-driven production of hydrogen peroxide requires a thorough knowledge of the main redox couples involving O_2, H_2O, and H_2O_2 in aqueous solution:

$$O_{2(g)}+4H^+_{(aq)}+4e^- \rightarrow 2H_2O\ (1.23\ \text{V vs SHE}) \quad (6)$$

$$O_{2(g)}+2H^+_{(aq)}+2e^- \rightarrow H_2O_2\ (0.68\ \text{V vs SHE}) \quad (7)$$

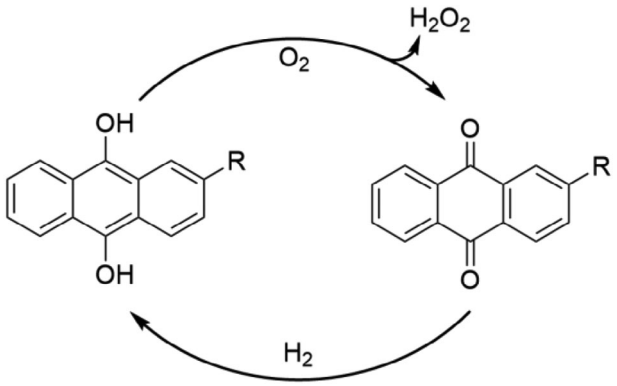


Figure 4. The industrial anthraquinone process.

$$O_{2(g)}+H^+_{(aq)}+e^- \rightarrow HOO^{\bullet}(-0.13\ \text{V vs SHE}) \quad (8)$$

$$H_2O_{2(aq)}+2H^+_{(aq)}+2e^- \rightarrow 2H_2O\ (1.77\ \text{V vs SHE}) \quad (9)$$

$$2H^++2e^- \rightarrow H_{2(g)}\ (0.00\ \text{V vs SHE}) \quad (10)$$

It is important to note that all these reactions are highly pH-dependent. Therefore, the redox potential must be appropriately calculated depending on the reaction conditions. Indeed, the thermodynamic potentials can vary by several hundred millivolts between acidic and alkaline environments. For example, the $2e^-$ ORR (Equation 7) to H_2O_2 is significantly less spontaneous at pH 7, with a redox potential as low as 0.27 V. Although it is common practice to evaluate the activity and selectivity of a semiconductor photocatalyst by comparing the position of its conduction and valence bands to reduction potentials, these are sometimes erroneously taken at their reference state, that is at an impractical pH = 0.

Hydrogen peroxide was first generated by electrolysis, but since the 1940s, it has been produced on a large scale through the so-called "anthraquinone process" (**Figure 4**). In this method, a 2-alkyl anthraquinone is first reduced to the corresponding hydroquinone using hydrogen gas over a Pt catalyst. Hydroquinone is then oxidized back into air, and as a result, O_2 is reduced to H_2O_2, and the cycle is repeated.[76,77] Despite its high yield, the process has several drawbacks: i) the use of pressurized H_2, ii) the need for a noble catalytic metal, iii) the generation of by-products from parasitic anthraquinone ring hydrogenation, and iv) the need for a liquid-liquid extraction step to isolate H_2O_2 from the organic phase. Such limitations urged scientists to find innovative and sustainable electrocatalytic or direct photocatalytic methods for H_2O_2 generation.[78] Furthermore, it is worth highlighting that the H_2 input commonly used in the chemical industry is fossil-derived H_2 (grey hydrogen).

In the context of light-driven synthesis, many catalytic materials have been tested, including metal oxides, metal-organic frameworks, and carbon nitrides.[79] Photocatalytic production of H_2O_2 has been almost entirely concerned with ORR. While H_2O_2 can be successfully synthesized in good yields using a variety of materials, several challenges still need to be addressed for a viable large-scale alternative. Some of the issues to be tackled are common to all photocatalysts: light-absorption should be enhanced in order to utilize a larger portion of sunlight, charge

 © 2023 The Authors. Global Challenges published by Wiley-VCH GmbH

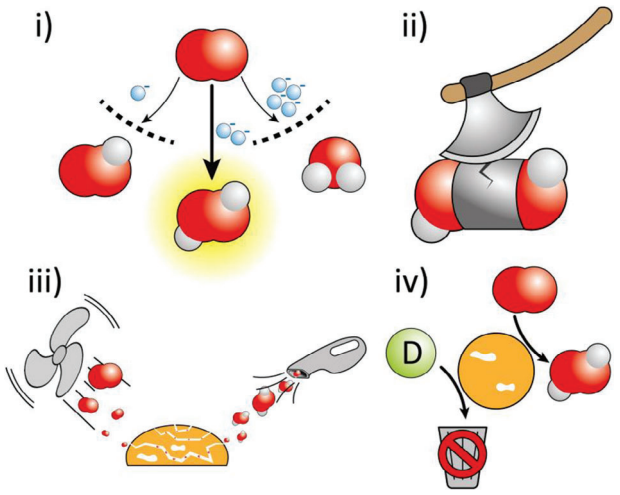


Figure 5. Challenges to be addressed for developments in sustainable H_2O_2 synthesis. i) Enhanced selectivity toward $2e^-$ ORR to H_2O_2; ii) Suppression of H_2O_2 decomposition; iii) Improved mass transfer of reactants and products; iv) Alternative solutions to sacrificial electron donors.

separation efficiency should be increased, and charge recombination should be suppressed as much as possible.[80] However, challenges more specifically associated with H_2O_2 synthesis can be identified (**Figure 5**):

(a) Selectivity of ORR should be increased: Oxygen can be either reduced through a $4e^-$ (Equation 6), $2e^-$ (Equation 7), or $1e^-$ (Equation 8) route, yielding H_2O, H_2O_2 and HOO·, respectively. Trade-offs between thermodynamics and kinetics can be identified. The first reaction is thermodynamically favored, but it requires a kinetically challenging 4-electron transfer. On the other hand, the generation of hydroperoxyl radicals has a much lower reduction potential, but it can rapidly occur by a single electron transfer. Moreover, for a reductive enough photocatalyst, the $1e^-$ route will dominate in most scenarios. Nominally, for ideal ORR selectivity toward H_2O_2, the conduction band of a photocatalytic semiconductor (or, equivalently, the lowest unoccupied molecular orbital of a molecular catalyst) should lie between the reduction potential of (Equation 7) and (Equation 8), that is between −0.54 V and 0.27 V versus SHE at pH 7, or −0.13 V and 0.68 V at pH 0. As illustrated in the following section, selectivity can also be shifted with different strategies, for example working on the morphology of the catalyst to favor adsorption of transient species.[81]

(b) Decomposition of synthesized H_2O_2 should be suppressed: Hydrogen peroxide is susceptible to disproportionation to H_2O and O_2 even at mild conditions. This reaction can even be accelerated in the presence of transition metals. In the design of metal-based catalysts for ORR, it is crucial to ensure that synthesized hydrogen peroxide is not decomposed in-situ on the same material. For example, Ag is well-known to catalyze H_2O_2 disproportionation.[82] More studies suggest that Pt and Pd lead to even faster decomposition rates, followed by Au.[83] In addition to the material, the illumination source also plays a major role. UV light is known to cleave the peroxide bond.[84] Consequently, the use of band-pass filters to avoid shorter wavelengths is highly recommended. For the same reason, systems relying on TiO_2 excitation should be evaluated with care, since a remarkable conversion of O_2 might still result in low H_2O_2 yields because of its UV-induced degradation to radicals.

(c) Mass transfer of O_2 should be improved: In an aqueous solution, the extent of ORR is dictated by the liquid-air contact area and the concentration of dissolved gas. Oxygen is usually bubbled to increase the reaction yield, but once the dissolved gas is consumed, mass transfer may become the limiting step of the reaction. It should be remembered that oxygen solubility in water at room temperature and 1 atm is ≈1.22 mmol L^{-1}.[85] Strategies to overcome this issue might involve multiphasic systems or gas diffusion layers.

(d) The reaction ideally should occur without any sacrificial electron donor: This last challenge will probably be the hardest to address. Indeed, most reports on photocatalytic H_2O_2 synthesis rely on alcohols or amines as sacrificial electron donors. Smarter electron-donating substrates might be chosen, in the view of a circular economy. For example, glycerol waste from biofuel synthesis[86] or ethylene glycol from PET recycling are valid reducing substrates.[87] In an ideal scenario, H_2O_2 should be produced from the convergence of $2e^-$ ORR and WOR (comproportionation). However, the latter is a surprisingly thermodynamically challenging reaction, often replaced by $4e^-$ oxidation to O_2, with an admittedly very sluggish kinetics. $2e^-$ WOR has been scarcely reported, mainly in electrochemical devices,[88] and therefore deserves more consideration.

In the following paragraph, possible approaches to each of these challenges will be provided with reference to the state-of-the-art.

3.1. Approaches to Light-Driven H_2O_2 Production

Selective synthesis of hydrogen peroxide is commonly achieved through careful band engineering, particularly for the ORR scenario, the conduction band should not lie at too negative potentials to prevent the formation of HOO· species. In general terms, band engineering is achieved by hybridization of the native catalyst with a variety of materials. We have summarized the most relevant photocatalyst employed for H_2O_2 production through both WOR and ORR pathways (**Table 2**).

Covalent functionalization has been extensively investigated for graphitic carbon nitrides.[89] While these materials are safe, inexpensive, and responsive to visible light, they are non-selective and not exceptionally active due to charge recombination. Protocols are available for the covalent attachment of carbon nitrides to carbon-rich materials like carbon nanotubes,[90] or charge-separating centers like polyoxometalates.[91] On the other hand, $BiVO_4$ has intrinsically ideal band positions for the selective $2e^-$ ORR, with its conduction band approximately located at 0.02 V versus SHE.[92] It is inexpensive and possesses a low bandgap (≈ 2.5 eV) compatible with the absorption of visible light. Nevertheless, it needs catalytic materials to improve chemical conversion.

 © 2023 The Authors. Global Challenges published by Wiley-VCH GmbH

Table 2. Summary of different photocatalysts applied for H_2O_2 production.

Catalyst	Mechanism	Catalyst mass [mg]	Light wavelength [nm]	H_2O_2 rate [μmol g^{-1} h^{-1}]	AQY [%]	Ref
CDs@CTFs	ORR/WOR	30	Sunlight simulator	≈633.3	0.93% (505 nm)	[80]
g-C_3N_4	ORR	20	420–500	125	0.07 (375 nm)	[81]
Au/WO_3	ORR	50	420	18.7	N/A	[83]
PCN-NaCA	ORR	10	Sunlight simulator	1870	27.6 (380 nm)	[86]
g-C_3N_4-CNTs	ORR/WOR	50	420–700	658	N/A	[90]
$Au_{0.2}$/$BiVO_4$	ORR	50	>420	2412	0.24 (420 nm)	[93]
H-PHI	ORR	5	410	1556	0.86	[95]
MIL-R7	ORR	5	>420	≈1073	N/A	[96]
TiO_2	ORR	30	300 or 420	719.5 (300 nm)	N/A	[102]
Sb-SAPC15	ORR/WOR	100	400–500	91 149	17.6 (420 nm)	[103]
Co_1/AQ/C_3N_4	ORR	6	Xenon lamp	57.5	0.054%[a)]	[105]
TiO_2	ORR	50	280–400	335	29.1% (334 nm)0.5 (Xe lamp)	[106]
g-C_3N_4/PDI-$BN_{0.2}$-r$GO_{0.05}$	WOR	50	420–500	74	7.3 % (420 nm)	[107]

[a)] Full spectrum.

The most viable catalytic materials are noble metal nanoparticles, as was demonstrated with Au (**Figure 6**a,b).[93]

Nevertheless, certain photocatalysts can shift the ORR selectivity toward H_2O_2 by lowering the adsorption energy of key intermediates. This surface chemistry effect was first demonstrated for carbon nitrides in Shiraishi's group which detected a 1,4-endoperoxide species on the surface of carbon nitrides by means of Raman spectroscopy.[81] The full mechanism is described in detail in the following paragraph.

In H_2O_2 synthesis, selectivity is often overlooked, and the performance of a photocatalytic method is primarily evaluated in terms of the yield or rate of hydrogen peroxide production. However, from this approach, many photocatalytic materials might be discarded because deemed as inactive, while in fact, they could only lack selectivity. To resolve this uncertainty, it is highly recommended that authors consider an electrochemical Koutecky-Levich analysis.[94] This analysis is performed on a rotating disk electrode (RDE) and can easily provide information on the average number of electrons transferred from the catalyst to the substrate, with fast experimental procedures and minor data analysis required, provided that the catalyst is successfully deposited on the working electrode. The technique consists of recording

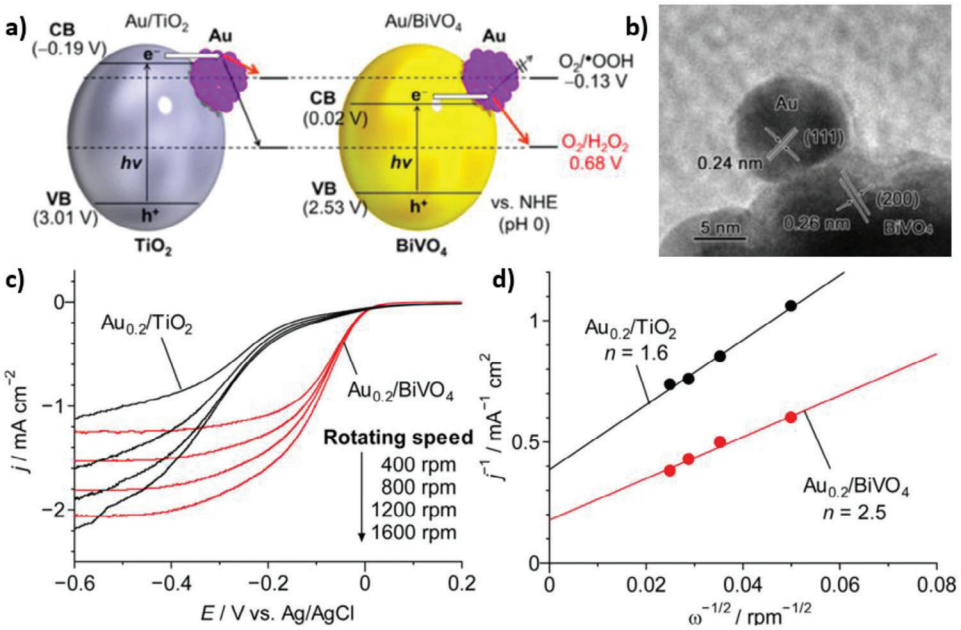


Figure 6. a) Illustration of Au/TiO_2 and $Au/BiVO_4$ photocatalysts with relevant band energies and reduction potentials. b) High-resolution transmission electron microscopy (HR-TEM) of $Au/BiVO_4$. c,d) Koutecky-Levich analysis of two ORR photocatalysts. c) Linear-sweep voltammograms measured on a rotating disk electrode at different rotating speeds. d) Koutecky-Levich plots at the constant potential of −0.3 V versus Ag/AgCl. Reproduced with permission.[93] Copyright 2016, American Chemical Society.

 © 2023 The Authors. Global Challenges published by Wiley-VCH GmbH

linear-sweep voltammetry data in an RDE at different rotating speeds. The inverse of the current density at a constant voltage is then plotted against the inverse of the square root of the rotating speed and fitted by linear regression. The number of electrons transferred in the redox process can be determined by the slope of such a plot, using the following relationships:

$$j^{-1} = k + B^{-1}\omega^{-\frac{1}{2}} \quad (11)$$

$$B = 0.2nF\nu^{-\frac{1}{6}}CD^{\frac{2}{3}} \quad (12)$$

where k is a constant, j is the current density, w is the rotating speed, n is the average number of transferred electrons, F is the Faraday constant, n is the kinetic viscosity of water (0.01 cm^2 s^{-1}), C is the concentration of O_2 in solution and D is the diffusion coefficient of O_2. A Koutecky-Levich analysis was performed for the $Au/BiVO_4$ photocatalyst and compared to Au/TiO_2 (Figure 6c,d).[93] The slopes of the j^{-1}-$\omega^{-1/2}$ curves for the two catalysts at a relevant potential resulted in n values of 2.5 and 1.6, respectively. The result indicated that $Au/BiVO_4$ has a role in promoting the $2e^-$ ORR, while with Au/TiO_2 the $1e^-$ pathway dominates.

Once H_2O_2 is selectivity produced, care should be taken to prevent its decomposition due to its very spontaneous disproportionation. Even though H_2O_2 is synthesized with remarkable selectivity, final yields might be low due to *in-situ* degradation on the catalyst. For example, poly (heptazine imides) (PHI) single-atom photocatalysts comprising a variety of noble and abundant transition metals were recently tested for photocatalytic ORR. Surprisingly, the best activity was achieved with the supposedly non-catalytic Na-PHI precursor.[95] Indeed, it was observed that when fresh H_2O_2 was mixed with a transition-metal single-atom catalyst – namely Fe-PHI – it was consumed faster than on Na-PHI, with the rate of decomposition increasing with the metal loading. Noble metals are particularly problematic catalysts. In particular, Pt, Pd, and Ag should be avoided, because of their demonstrated high rate of H_2O_2 decomposition.

To address this issue, alternative strategies can be adopted to facilitate the fast and efficient desorption of the product from the catalyst. This was demonstrated in a biphasic system, where a hydrophobic photocatalyst was dispersed in an organic phase, while hydrogen peroxide was concentrated in water.[96] This strategy also mimics the industrial anthraquinone process, where H_2O_2 is extracted in an aqueous solution after reaction in the organic phase. Triphasic systems might particularly improve the reaction since they address both product desorption and enhanced gaseous reactant mass transfer. Instead of organic solvents, oxygen might be conveyed to the catalyst through porous substrates on which a wet layer of photocatalyst is deposited (**Figure 7**). Microporous geometries are especially beneficial for increasing the contact area between the gas and the solid-liquid phase.

However, there are only a few examples of micro-engineered gas diffusion layers for ORR. In one of the reported attempts, a melamine foam was chosen as a porous substrate and as a support for photocatalytic graphitic carbon nitrides. Faster gas diffusion to the reaction center led to a 10-fold increase in H_2O_2 production over the traditional biphasic system.[97] In general, for triphasic reactors, it is fundamental to design hydrophobic catalysts. Hydrophobicity will not only favor H_2O_2 desorption but will also ensure the high stability of the catalyst at the liquid/air interface. Materials whose chemical composition can be tuned through bottom-up approaches like covalent organic frameworks (COFs) are good candidates for this purpose.[98] Reticulate materials including metal-organic frameworks are also characterized by high surface area for improved reactant/product diffusion.

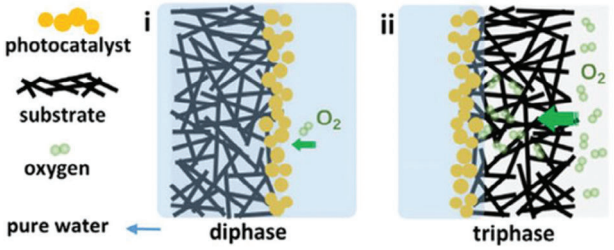


Figure 7. Schematic illustration of i) a biphasic and ii) a triphasic reactor for catalytic H_2O_2 synthesis. Reproduced with permission.[98] Copyright 2021, John Wiley and Sons.

Finally, ORR admittedly still strongly relies on organic alcohols or amines as sacrificial electron donors. The whole field of photoredox catalysis needs a paradigm shift from the convenient but wasteful optimization of half-reactions to the co-valorization of both oxidation and reduction sides. The latter perspective has risen in recent years under the name of "photoreforming". Although this is majorly referred to as biomass valorization,[99] a whole range of non-sacrificial electron donor substrates exists. These include ethylene glycol from plastic bottle recycling,[100] glycerol from the synthesis of biodiesel,[86] 5-hydroxymethylfurfural (HMF) from the degradation of various biomass-derived substrates.[101]

3.2. Proposed Mechanisms for Light-Driven H_2O_2 Synthesis

Clarifying the chemical pathways of hydrogen-oxygen combination in either ORR or WOR is fundamental for the design of photo and electrocatalysts with enhanced selectivity for hydrogen peroxide. The mechanism of the anthraquinone process is well-understood and it is known to proceed via a radical autoxidation in which intermediate HOO· species are generated as a result of hydrogen atom transfer (HAT) from hydroquinone by dioxygen. Two subsequent HATs lead to H_2O_2 and the oxidized anthraquinone.[77]

Carbon nitrides are excellent catalytic substrates for $2e^-$ ORR thanks to the formation of a favorable 1,4-endoperoxo species on triazine units. This labile intermediate first detected with Raman spectroscopy by Shiraishi et al. is expected to be key to suppressing $1e^-$ ORR to hydroperoxyl radicals.[81] Through the formation of the peroxo bridge, two oxygen atoms can receive two electrons and two protons simultaneously and directly from the C_3N_4 scaffold (**Figure 8**a). The two electrons are supposed to be localized at the C1 and N4 positions of the triazine ring, while holes are at the N2 and N6 positions. Once the holes oxidize an electron donor (such as CH_3OH), oxygen is reduced generating a peroxo species. While this intermediate would generally be protonated and released as HOO·, the proximity of a highly reducing electron on the triazine kinetically favors the formation

 © 2023 The Authors. Global Challenges published by Wiley-VCH GmbH

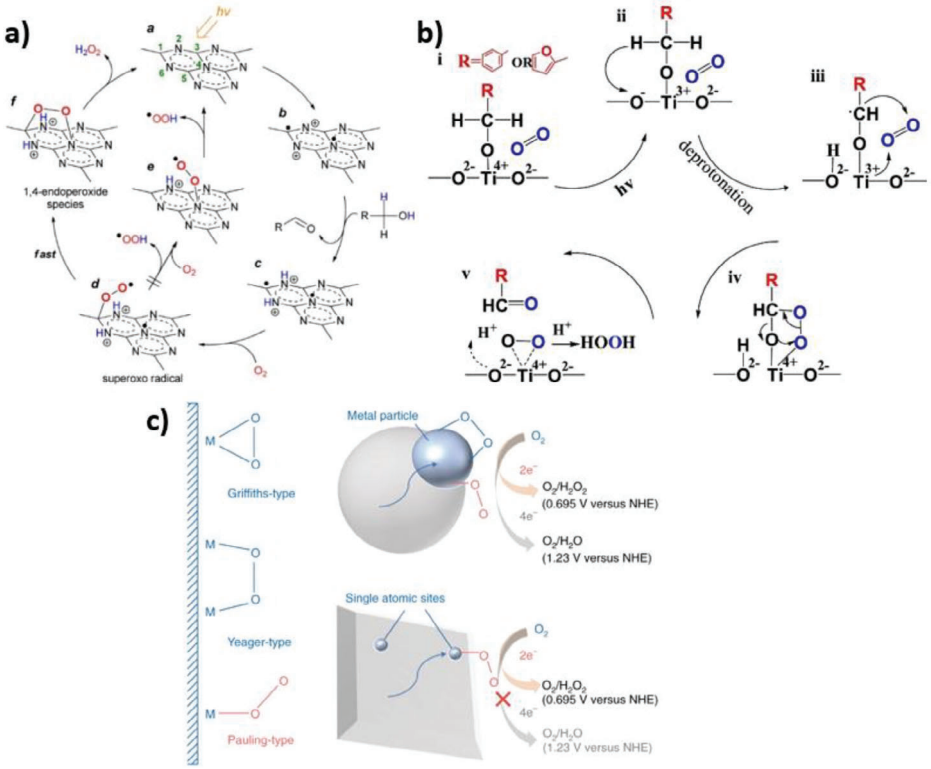


Figure 8. a) Scheme of the proposed mechanism of selective 2e⁻ ORR on C_3N_4. Reproduced with permission.[81] Copyright 2014, American Chemical Society; b) Scheme of the proposed mechanism of selective 2e⁻ ORR on TiO_2 using aromatic alcohols as electron donors. Reproduced with permission.[102] Copyright 2020, Elsevier; c) Illustration of the edge-on and end-on absorption of O_2 on catalysts and suppressed 4e⁻ reduction on single atoms. Reproduced with permission.[103] Copyright 2021, Springer Nature.

of the 1,4-endoperoxide, and thus the subsequent protonation and desorption as H_2O_2.

A similar involvement of peroxo species was proposed for TiO_2-photocatalyzed H_2O_2 production (Figure 8b).[102] Here, electron-donating deprotonated alcohols form a complex with surface Ti^{IV} centers. Upon UV irradiation, titanium is reduced to Ti^{III} and then a hydrogen atom is transferred from the alcohol to a surface oxygen atom, yielding an alkyl radical. Dioxygen swiftly binds to this reactive species and to Ti, resulting in a five-membered ring intermediate. Finally, bonds rearrange resulting in an aldehyde and a cyclic Ti-O-O peroxide, which is selectively converted to H_2O_2 by double protonation. Such a mechanism was proposed for aromatic alcohols, which better stabilize the alkyl radical intermediate. The chemical adsorption of alcohols is also beneficial in inhibiting UV-catalysed hydrogen peroxide decomposition on TiO_2.

Recently, mechanistic advances reported by Ohno and coworkers suggested that single-atom catalysts (SACs) might have a great potential to suppress 4-e⁻ ORR to water.[103] Conversion of O_2 to H_2O inevitably proceeds through the cleavage of the O-O bond. Oxygen can adsorb on ORR catalysts in different geometries that could favor or prevent bond scission, namely edge-on – including Griffiths-type and Yeager-type – and end-on, or Pauling-type (Figure 8c). The former – that incidentally pertains to the endoperoxide species described above – induces strain in the adsorbate structure so that the O-O bond is more likely to break. This configuration is common on metals or alloys, where all adjacent atoms are possible adsorption centers. Conversely, in SACs, catalytic atoms are isolated, so that dioxygen can only attach in an end-on fashion. Therefore, the scission of the two oxygen atoms is less favored, and conversion to water is suppressed. This was demonstrated on single-atom Sb supported on C_3N_4.[103]

As far as the WOR approach is concerned, more investigations are needed to unveil the most likely chemical pathways (**Figure 9**a). Catalyst design should focus on the fate of intermediate HOO· species generated from OH^-. If deprotonation is favored, then HOO· ends into the thermodynamically more stable O_2, but if protonation is instead enhanced – for instance kinetically from adsorbed H^+ – H_2O_2 is the preferred product. Nevertheless, efforts dedicated to 2e⁻ WOR should definitely start from the critical and unique HCO_3^--based catalysis. As illustrated in Figure 9b, percarbonate (HCO_4^-) ions were detected as key intermediates for the electrochemical oxidation of water to hydrogen peroxide.[104] It was proposed that bicarbonate ions first undergo step-wise 2e⁻ oxidation and addition to OH^-. It is therefore important to select anodes to enable efficient electron extraction from carbonate ions. In the future, applications for catalytic green H_2O_2 synthesis from the water will probably be in the form of electrocatalytic or photo electrocatalytic cells, with HCO_3^- anolytes constituting a fundamental component.

Overall, it can be concluded that major advances in sustainable hydrogen peroxide production will come from systems capable of combining ORR and WOR in a single clean and non-sacrificial

 © 2023 The Authors. Global Challenges published by Wiley-VCH GmbH

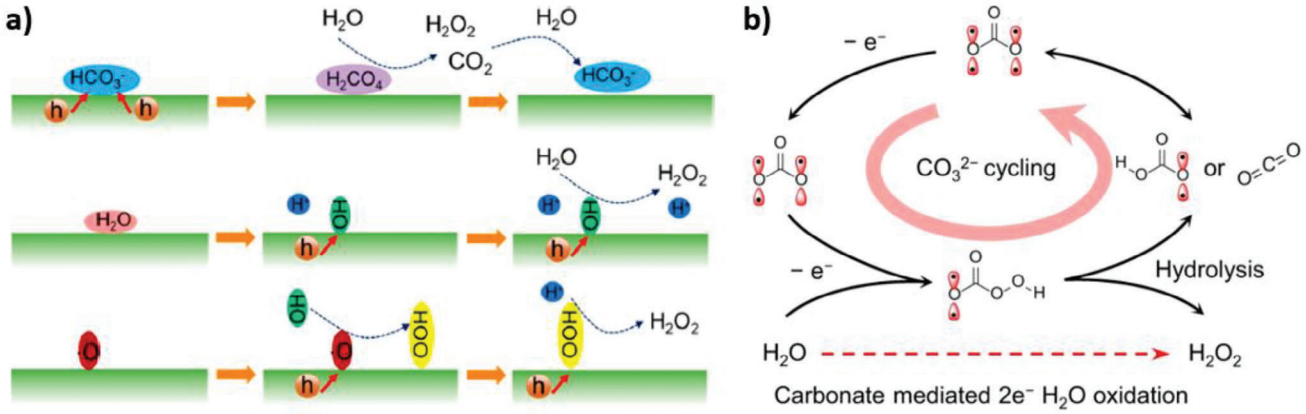


Figure 9. a) Schemes of proposed mechanisms for 2e⁻ WOR. Reproduced with permission.[88] Copyright 2019, American Chemical Society; b) Scheme of proposed mechanism for HCO_3^--assisted H_2O_2 electrochemical synthesis. Reproduced with permission.[104] Copyright 2022, Springer Nature.

dual-cycle. Few attempts have been successfully proven, so far. A possible approach consists of including isolated oxidative and reductive centers on a common substrate. This strategy was demonstrated by Kim et al. in the combination of reducing Co single atoms and oxidizing grafted anthraquinone molecules on a C_3N_4 support.[105] Despite the ideal photocatalytic process coupling ORR and WOR still far from the efficiency displayed by the commercial fossil-based H_2O_2 anthraquinone process, the H_2O_2 photocatalytic production deserves the spotlight in terms of solar to chemical approach. The photocatalytic production of H_2O_2 in some optimized conditions, for example, employing sacrificial reagents (e.g., biomass-derived molecules or wastes) can display impressively high H_2O_2 production rates.[95] State-of-the-art TiO_2 achieved a remarkable H_2O_2 production rate of 3.3 mM h^{-1}, although requiring illumination at shorter wavelengths (> 280 nm) and benzyl alcohol as an electron donor,[106] but a very similar performance was demonstrated with C_3N_4 composites including pyromellitic diimide (PDI) and reduced graphene oxide (rGO) in the presence of widely available ethanol.[107] Both these materials also achieved remarkable apparent quantum yields (AQY) of 29% and 7%, respectively. In this sense, this process might be one of the examples of direct use of photocatalysis in a solar-to-chemical approach, closest to reaching the efficiency required to be commercially used. Certainly, more advances are still needed, as well as investigations about the economic feasibility. However, it is worth highlighting the potential of this technology, which might be disruptive to the production of an important chemical responsible for an important consumption of fossil-derived H_2.

4. Photocatalytic-driven Hydrogenation

Another crucial aspect of the industrial chemical transformation is the reduction of organic compounds. This particular field stands out as one of the most prevalent in industrial reactions, with an estimated 25% of all industrial processes incorporating at least one hydrogenation step.[108,109] In addition to its extensive application in fine chemicals and pharmaceuticals, hydrogenation is also widely employed in petrochemicals, particularly during hydrodenitrogenation and hydrodesulfurization steps.[110]

Traditionally, the industrial sector has made use of noble metals as catalysts and molecular hydrogen as the primary agent for reducing unsaturated bonds, such as C═C, C═N, and C═O, this approach is not only expensive due to the rarity of the noble metals, but also hazardous for the high pressures and temperatures of operation. In recent times, a new approach to hydrogenation has gathered attention, known as transfer hydrogenation. This strategy involves an alternative hydrogen donor for the reduction process without the employment of H_2 gas. Transfer hydrogenation offers unique advantages by providing opportunities for a more sustainable process, readily available, inexpensive donors, and its versatility, as it avoids the challenge associated with H_2 storage and production. Typically, this reduction is conducted catalytically and driven by thermal or light energy.

Nevertheless, several studies have demonstrated the high potential of photocatalytic systems in comparison to the thermal pathway. Beyond its compelling sustainability proposition, photohydrogenation offers highly efficient and inherently more energetically favorable reaction mechanisms that outperform traditional thermal pathways,[111] reducing the reliance on fossil-derived hydrogen (**Figure 10**). One of the key advantages of photocatalytic transfer hydrogenation is the ability to harness solar energy for the reduction process, making it a sustainable and environmentally friendly approach. Additionally, the controlled application of moderate heat in combination with photohydrogenation can lead to synergistic effects, further improving reaction efficiency and selectivity.[112]

This provides the engineering of new catalysts with rationalization capabilities to design and produce highly efficient systems, wherein hot photogenerated charges are the reduction sites within the process. This session will delve into the multitude of advantages and promising prospects offered by tailored photocatalytic processes, specifically aimed at transfer hydrogenation reactions. In other words, the photocatalytic hydrogen transfer reaction is a perfect example of the direct use of green hydrogen through a solar-to-chemical strategy. We have also compiled a set of the most influential works involving hydrogen transfer reactions using photocatalysts (**Table 3**).

Moving away from H_2 as a chemical feedstock for organic synthesis is not a trivial task, as performing hydrogenations with

 © 2023 The Authors. Global Challenges published by Wiley-VCH GmbH

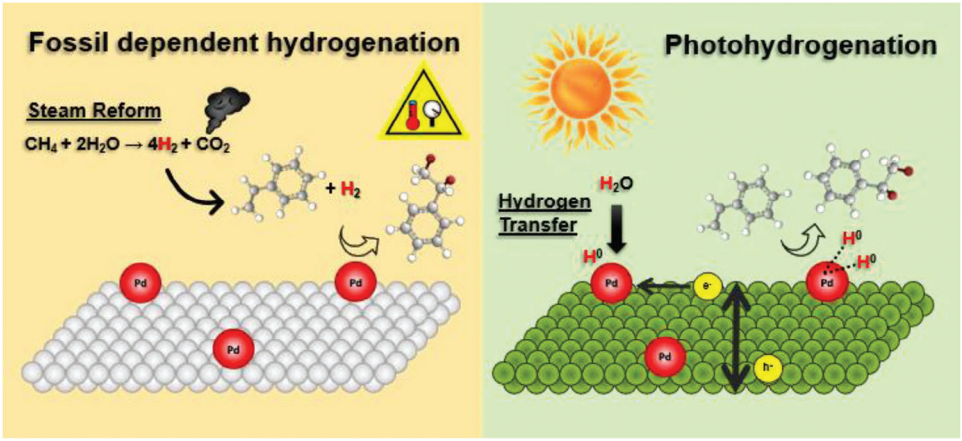


Figure 10. Comparative illustration between the industrial hydrogenation process, which relies on molecular hydrogen derived from methane reforming, and the photocatalytic process utilizing hydrogen transfer from water as an alternative source.

H_2 offers a perfect atom efficiency reaction. Regardless, the current need for reactions in mild conditions and with green hydrogen sources has pushed research toward alternative hydrogen sources. Several types of sacrificial donors and catalytic systems have been studied as hydrogen sources for transfer hydrogenation reactions.[109,113] In these cases, for the chemical species to be considered as relevant substitutes for H_2 in large-scale applications, they must be cheap, easy to transport, stable, and renewable. Additionally, they must be paired with highly active catalysts to have competitive processes that could pose as a viable route for hydrogenation.

One promising class of compounds that can be employed as hydrogen sources in H-transfer reactions are organic molecules derived from biomass (e.g., alcohols, and carboxylic acids). They possess low toxicity and are widely available and cheap. Small-chain alcohols such as methanol and ethanol have been previously used in semihydrogenation of alkynes, with great control in selectivity. For instance, Jia et al. supported nickel nanoparticles on a carbon nitride scaffold, which was successful in the photocatalytic semihydrogenation of phenylacetylene into styrene, with selectivity >90% over several usages.[114] Meanwhile, Su and coworkers demonstrated that by inducting modifications in structure of an Nb_2O_5 support and the Pt species on it, they could control the products in the photoreduction of phenylacetylene. On Pt/2D Nb_2O_5 hydrogen transfer from ethanol led to styrene as the major product, while Pt/Bulk Nb_2O_5 was more selective to H_2 evolution.[115] Isopropanol has also been used as a hydrogen source in the reduction of nitroarenes in the work of Deng et al. The authors used non-noble Fe-based photocatalysts (Fe/C_3N_4) in which iPrOH was oxidized into acetone and nitrobenzene reduced into acetone with no reported H_2 evolution.[116]

Formic acid (FA) is regarded as one of the best hydrogen carries in terms of gravimetric capacity, safety, and cost.[117] Tsutsumi et al. have demonstrated a photocatalytic system utilizing

Table 3. Summary of different photocatalysts applied for transfer hydrogenation of unsaturated bonds.

Catalyst	Hole scavenger employed	Catalyst mass [mg]	Light wavelength [nm]	Target molecule/ product	Reaction time [h]	Conversion/ Selectivity [%]	Reference
Ni/C_3N_4	TEA	3	420	Phenylacetylene/Styrene	14	100 (97)	[114]
Pt/Nb_2O_5-A	EtOH	10	365	Phenylacetylene/Styrene	10	≈60 (N/A)	[115]
Fe/g-C_3N_4	i-PrOh (10%)	20	365	Nitrobenzene/Aniline	3	100 (100)	[116]
Pd/Si	HCOOH	25	375–800	Nitrobenzene/Aniline	3	100 (99)	[118]
Au@ZrO_2	HCOOH	50	400–750	Phenylacetylene/Styrene	16	100 (25)	[119]
Pt/g-C_3N_4	TEA (10%)	30	420	HMF/DHMF	4	0.457 h^{-1} (TOF)[a]	[122]
Pd-mpg-C_3N_4	H_2O	10	427	Styrene/Ethylbenzene	10	100 (100)	[124]
Ni-N/CN	H_2O	20	420	2-Ethynylnaphthalene/ 2-vinylnaphthalene	2	100 (98)	[125]
Pd/TiO_2	Glucose	25	350	4-nitroacetophenone/ 4-aminoacetophenone	12	99 (99)	[126]
TiO_2/Ce_2S_3	H_2O	15	365	Nitrobenzene/Aniline	1.5	100 (99)	[127]
LCN	H_2O	20	420	4-nitrophenol/4-aminophenol	1.67	96.5 (98.9)	[128]

[a] Turnover frequency (TOF).

 © 2023 The Authors. Global Challenges published by Wiley-VCH GmbH

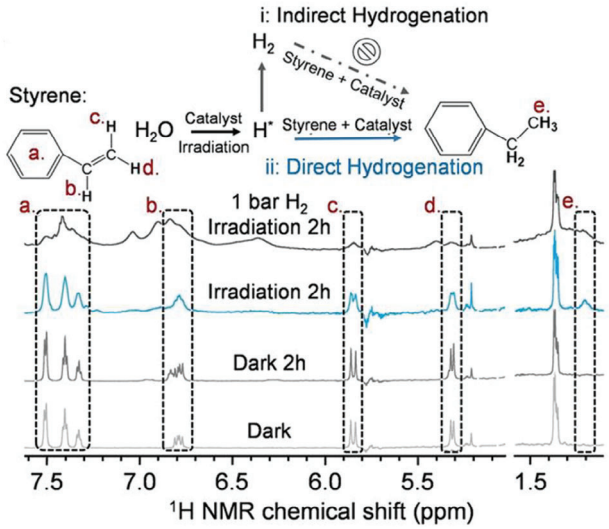


Figure 11. Operando ^{1}H-NMR of the photocatalytic water transfer hydrogenation of styrene induced by the photocatalyst Pd_1-mpg-C_3N_4. Reproduced with permission.[124] Copyright 2022, John Wiley and Sons.

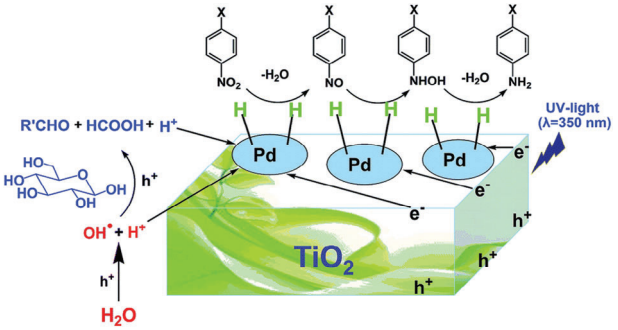


Figure 12. Proposed reaction pathway in the selective photocatalytic transfer hydrogenation of nitroarenes into anilines by an H_2O/glucose system catalyzed by Pd/TiO_2. Reproduced with permission.[126] Copyright 2016, Royal Society of Chemistry.

a Pd/Si hybrid material for the reduction of several nitroarenes in ambient conditions with great yields.[118] Another great example was demonstrated by Huang et al. where FA was successfully employed in the reduction of nitroarenes, olefins, aldehydes, imides, and alkynes, by the photocatalytic activity of Au@ZrO_2 nanocatalyst.[119]

Water would be regarded as the most ideal hydrogen source for transfer reactions; however, the reaction pathways are usually impeded by the energy-demanding and kinetic hindered water oxidation reaction. Luckily, the attractiveness of this approach has led to intensive research in the past years, and significant progress has been made in this field by both homogeneous and heterogeneous photocatalysts.[120,121] In 2016 Guo et al. managed to demonstrate a photocatalytic system where Pt/g-C_3N_4 catalyst was able to reduce water into hydrogen and subsequently utilize the H_2 for the reduction of HMF into DHMF.[122] There are many cases where hydrogen is directly consumed in the reaction, in the form of H•.[123,124] This sophisticated approach was thoroughly investigated by Zhao and collaborators, in their work a Pd_1-mpg-C_3N_4 was used for the photo-induced hydrogenation of styrene by water. They monitored the progress of the reaction employing operando ^{1}H NMR and proved that no H_2 was being produced, instead protons where directly added to the molecule (**Figure 11**).[124] The selective semihydrogenation of alkynes by water-sourced proton was also explored in the work of Arcudi et al. by combining a heterogeneous photosensitizer of mpg-C_3N_4 and Co-TPPS as the catalytic site. The authors managed to convert acetylene into ethylene with 99% selectivity even in competitive conditions (ethylene co-feed).[121] Meanwhile, Jie et al. managed to carry the deuteration of several alkynes into their respective alkenes using D_2O as a D-source using Ni-N/C_3N_4 photocatalyst under ambient conditions and with great selectivity.[125]

The synthesis of anilines is of great industrial significance, a green and renewable route is highly desirable. Taking that into account, Zhao and coworkers developed a Pd/TiO_2 photocatalyst capable of a transfer hydrogen reaction. In their work, a water/glucose solution was used as an H-source for the reduction of several nitroarenes under UV-light. The results showed that both glucose and water acted as H-sources (**Figure 12**), with water being responsible for ≈24% of hydrogen delivery.[126] In another work, Xu et al. utilized TiO_2 support with Cd_2S_3 nanoparticles for direct nitrobenzene reduction by water, in their most optimized condition, their hybrid photocatalyst was capable of producing aniline at 99% selectivity under 90 minutes.[127] A carbon nitride-based catalyst was also investigated in this type of reaction by Yao et al. In their work, p-nitrophenol was reduced into p-aminophenol by Pt/C_3N_4 and water, while simultaneously H_2 was also being produced by the water splitting reaction. The authors combined the use of DFT calculations and isotope labeling to prove that H° coming from water was the reactive species for the reduction.[128]

Deuterium labeling in organic molecules is another chemical transformation of great interest due to the kinetic isotope effect, allowing investigation of reaction mechanisms,[129] modification of selectivity,[130] and change in physical-chemical properties that can be exploited for pharmaceutical compounds.[131] In that sense, transfer deuteration from water offers a direct and waste-free synthetic approach for high-end fine chemicals. Aryl halides are the most common substrates for this kind of transformation,[132–134] for instance, Liu et al. used a porous CdSe photocatalyst for the deuteration of different classes of aryl halides. The photocatalytic system was even capable of deuteration of C—Cl and C—F bonds with selectivity yields >90%.[133] Another great example of deuteration of the highly stable C-Cl bonds has been demonstrated by Ling et al., where Pd nanosheets supported on crystalline polymeric carbon nitrides (CPCN) were able to induce the deuterium transfer form D_2O using triethanolamine (TEOA) as a sacrificial reagent, without leading to reduction or hydrogenation of other functional groups.[132] Besides aryl halides, diaryl alcohols, and carbonyl are also viable choices of substrate for transfer deuteration,[135] Nan and coworkers managed to utilize diaryl alcohols as substrate for deuterated water transfer reactions. Their approach involved the usage of CdSe quantum dots under ambient conditions and visible light irradiation. This reaction system was successful in the deuteration of a great scope of substrate with good yields.[136]

 © 2023 The Authors. Global Challenges published by Wiley-VCH GmbH

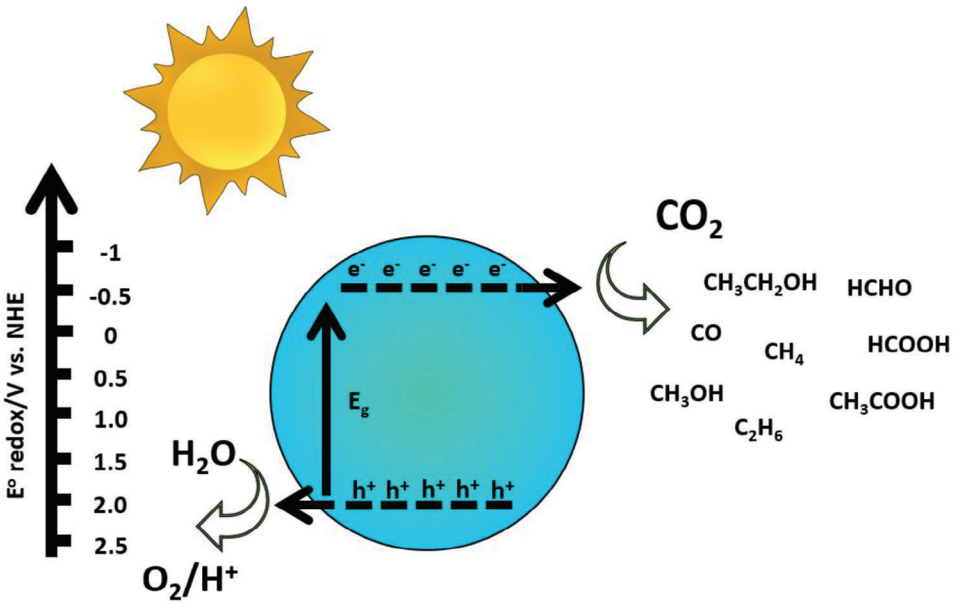


Figure 13. Diagram representing the photoreduction of CO_2 using water as electron donor.

5. Photocatalytic-driven CO_2 Reduction

Our strong reliance on fossil fuels gives rise to innumerable challenges. Not only are they finite resources, but their combustion exerts a deep impact on the sustainability and thermal equilibrium of our planet.[137] Carbon dioxide stands out as a primary driver of these anthropogenic transformations, attracting great efforts toward the development of new strategies and technologies aimed at mitigating its occurrence and reducing atmospheric concentrations. Despite the environmental concerns surrounding it, CO_2 is widely recognized as an optimal feedstock for the conversion into C_1 and C_{2+} high-demand chemicals.[138–140] Various catalytic processes, including CO_2 hydrogenation, Fischer-Tropsch, water-gas-shift, and reverse-water-gas-shift represent the primary routes for carbon valorization. Conventionally, these processes are performed utilizing fossil-derived H_2 as a reductive agent and expensive supported metal catalysts operating under harsh conditions.[140] CO_2 hydrogenations employing fossil-derived H_2 are not neutral in CO_2 emissions, once H_2 production by steam reforming or gasification holds an important CO_2 footprint. Hence, it is essential to develop new strategies to convert carbon dioxide to valuable chemicals employing green hydrogen sources).

More recently, in pursuit of a more environmentally friendly and feasible method, the scientific community has been making substantial efforts to mimic the natural photosynthetic process by exploring photocatalytic approaches induced by solar energy (**Figure 13**). Essentially, the photocatalytic CO_2 conversion presents fundamental limitations primarily associated with the high stability of the CO_2 molecule, low product selectivity, and slow kinetics involved in the multi-step reduction toward more complex products.[138,141] Moreover, the band structure of typical semiconductors is not adequate for simultaneous CO_2 reduction and H_2O oxidation, further challenging the process (See below the potential table measured at pH 7).[142] Nevertheless, remarkable progress has been made in this field, being close to the 10% efficiency required for artificial photosynthesis to be feasible.[143]

$$CO_{2(g)} + e^- \rightarrow CO_2^{\bullet -} (-1.90 \text{ V vs NHE}) \quad (13)$$

$$CO_{2(g)} + 2H^+_{(aq)} + 2e^- \rightarrow CO_{(g)} + H_2O_{(l)} (-0.53 \text{ V vs NHE}) \quad (14)$$

$$CO_{2(g)} + 2H^+_{(aq)} + 2e^- \rightarrow HCOOH_{(aq)} (-0.61 \text{ V vs NHE}) \quad (15)$$

$$CO_{2(g)} + 4H^+_{(aq)} + 4e^- \rightarrow HCHO_{(aq)} + H_2O_{(l)} (-0.48 \text{ V vs NHE}) \quad (16)$$

$$CO_{2(g)} + 6H^+_{(aq)} + 6e^- \rightarrow CH_3OH_{(aq)} + H_2O_{(l)} (-0.38 \text{ V vs NHE}) \quad (17)$$

$$CO_{2(g)} + 8H^+_{(aq)} + 8e^- \rightarrow CH_{4(aq)} + 2H_2O_{(l)} (-0.24 \text{ V vs NHE}) \quad (18)$$

$$2CO_{2(g)} + 8H^+_{(aq)} + 8e^- \rightarrow CH_3COOH_{(aq)} + 2H_2O_{(l)} (-0.31 \text{ V vs NHE}) \quad (19)$$

$$2CO_{2(g)} + 14H^+_{(aq)} + 14e^- \rightarrow C_2H_{6(aq)} + 4H_2O_{(l)} (-0.51 \text{ V vs NHE}) \quad (20)$$

The photoreduction of CO_2 remains a challenging reaction due to its inherent complexity. In essence, there are three primary obstacles that limit the progress of this reaction. Firstly, the adsorption and activation of CO_2 pose a significant challenge. Secondly, there are economic concerns associated with the use of expensive sacrificial reagents. Lastly, the formation of higher-value products, such as oxygenates, presents additional difficulties.

 © 2023 The Authors. Global Challenges published by Wiley-VCH GmbH

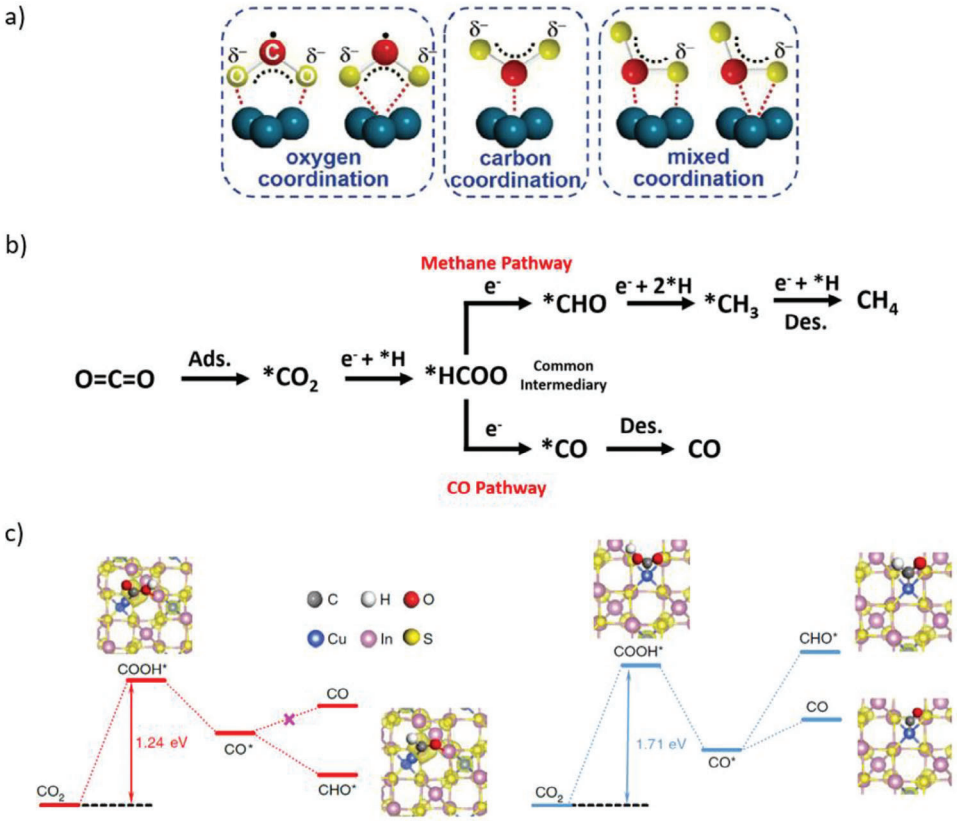


Figure 14. a) Schemes illustrating the three possibilities of CO_2 activation on the catalyst surface. Reproduced with permission.[146] Copyright 2020, Royal Society of Chemistry; b) Scheme representing the different pathways proposed for CO_2 reduction; c) Free energy of CO_2 reduction using dual-site Cu-In to manipulate the CO and CH_4 production induced by controlled sulfur structural vacancies. Reproduced with permission.[147] Copyright 2019, Springer Nature.

5.1. CO_2 Activation

Regarding the carbon dioxide activation, in photocatalytic systems, it is often observed that CO_2 molecules react with photogenerated electrons, leading to the formation of $CO_2^{\bullet-}$ species (Equation 13) that can undergo further conversions. This process is recognized as the rate-limiting step in photocatalytic CO_2 reduction reactions due to its associated high negative potential (−1.9 V vs NHE). To overcome this challenge, one strategy involves the adsorption of CO_2 molecules onto the surface of the photocatalyst, resulting in the formation of partially charged $CO_2^{\delta\bullet-}$ species.[144] This process effectively lowers the energy barrier for electron transfer, facilitating subsequent reactions.

Various reactive pathways to absorb CO_2 molecules have already been firmly established in the literature.[145] Due to the remarkable stability associated with the linear arrangement of the CO_2 molecule, the pivotal step involves breaking this linearity by activating the molecule during its interaction with the catalyst surface. The direct reduction of the gaseous phase CO_2 requires high reductive potential, making this process unfeasible (Equation 13). However, once chemisorbed in the active site of the photocatalyst, low energy potentials arise, turning the reaction kinetically more viable. Consequently, the catalyst design becomes an immensely crucial aspect to consider in CO_2 reduction, as it serves as a modulator for achieving a specific product. The diverse proposed mechanisms exhibit distinct characteristics depending on the geometry in which the CO_2 molecule is activated on the catalyst surface. Hence, following a specifical adsorption orientation, a series of successive electron transfer processes ensues (**Figure 14**b). Chemisorption can occur through three intriguing configurations (Figure 14a): i) pair acceptors, typically involving metals that interact with the lone pairs of terminal oxygen; ii) similarly, sites rich in electron density are capable of donating electrons to the vacant carbon orbitals, coordinating with them; iii) lastly, simultaneous coordination occurs through both carbon and oxygen atoms.

Several strategies have been developed to enhance CO_2 adsorption, including defect engineering involving oxygen, anion, and cation vacancies, surface modification, doping, and stabilization of single atoms (**Table 4**). Luo and Ji found that oxygen vacancies on TiO_2 exhibit higher activity in CO_2 reduction compared to surface Ti atoms.[148] This enhanced activity can be attributed to the combination of fast hydrogenation and deoxygenation pathways promoted by these lattice defects. The presence of oxygen vacancies in the lattice facilitates the deoxygenation of CO_2, leading to the formation of CO* or hydrogenation toward COOH* species. Dong and colleagues demonstrated that the introduction of Cu_2O onto ceria results in the creation of additional oxygen defects and Ce^{3+} sites, which play a crucial role in the deoxygenation of CO_2* to generate CO molecules.[149] The hydrogenation of

 © 2023 The Authors. Global Challenges published by Wiley-VCH GmbH

Table 4. Summary of different photocatalysts applied for CO_2 reduction.

Catalyst	Hole scavenger employed	Catalyst mass [mg]	Light wavelength [nm]	Main product	Rate conversion [μmol g^{-1} h^{-1}]	AQY [%]	Reference
2% CuCe	H_2O	50	Xenon lamp	CO	0138	N/A	[149]
BiOBr	H_2O	100	>400	CO	84.4	N/A	.[150]
V_S-$CuIn_5S_8$	H_2O	N/A	420-	CH_4	8.7	0.786[c)]	.[147]
5-T-Au/TiO_2	H_2O	10	Xenon lamp	CO	608	0.2 (380 nm)	[151]
Bi-OV-α-Ga_2O_3	H_2O	10	Xenon lamp	CO	42.3	N/A	[152]
RuP/C_3N_4	TEOA (20%)	8	>400	HCOOH	141 (TON)[a)]	5.7 (400 nm) 0.9 (420 nm)	[153]
RuRu′/Ag/C_3N_4	TEOA (20%)	4	Hg lamp	HCOOH	3110 (TON)[b)]	5.2 (400 nm)	[154]
Fe SAS/Tr-COF	TEOA	5	>420	CO	980.3	3.17 (420 nm)	[155]
Cu-CCN	CH_3CH_2OH	25	Xenon lamp	CO	3.086	N/A	[156]
OF-Co	TEOA (20%)	2	400-	CO	200.6	N/A	[157]
Ni-TpBpy	TEOA (20%)	10	>420	CO	915	0.3 (420 nm)	[158]
Ni-SA/ZrO_2	H_2O	10	Xenon lamp	CO	11.8	0.92% (365 nm) 0.36% (420 nm)	[159]
CoRu-HCNp	CH_3CH_2OH	25	Xenon lamp	CO	27.31	2.8% (385 nm)	[160]
α-Fe2O3/g-C_3N_4	H_2O	25	Xenon lamp	CO	27.2	0.49% (365 nm) 0.96% (420 nm)	[161]
0.33AB	H_2O	10	Xenon lamp	CO	212.6	N/A	[163]
P@U	H_2O	5	>420	HCOOH	146.0	N/A	.[164]
TTCOF-Zn	H_2O	100	420-	CO	2.05	N/A	[166]
TCOF-$MnMo_6$	H_2O	2	400-	CO	33.19	0.0067% (400 nm)	[167]
$BiOBr_{0.6}Cl_{0.4}$	H_2O	10	Xenon lamp	CO	15.86	N/A	[168]
Cu SAs/UiO6-NH_2	TEOA	100	>400	MeOH/EtOH	5.33/4.22	N/A	[169]
PTh/Bi_2WO_6	H_2O	50	>420	MeOH/EtOH	14.1/5.1	0.0086% (475 nm)	[170]
Co/g-C_3N_4.2 SAC	H_2O	5	Xenon lamp	MeOH	235.5	N/A	[171]
P/Cu SAs@CN	TEOA (10%)	≈0.5	Xenon lamp	MeOH	616.6	12.55% (350 nm)	[172]
$Ti_{0.91}O_2$-SL	H_2O	10	Xenon lamp	CO	67.0	0.48% (385 nm) 0.15% (415 nm) 0.06% (520 nm)	[173]
VS-SAL_{10}	H_2O	5	Xenon lamp	C_2H_4	44.3	0.51% (415 nm)[b)]	[174]

[a)] Values of turnover number (TON); [b)] External quantum efficiency (EQE); [c)] Full spectrum.

CO_2* molecules to COOH* species also contributes to the production of CO. Xie et al., for instance, developed BiOBr atomic layers with controlled oxygen vacancies and observed that the charge delocalization at these sites contributes to the formation of COOH* intermediates, which enhances the CO generation 20 and 24-fold than non-defect and bulk BiOBr, respectively.[150] Also, the introduction of desired defects could control the selectivity to other compounds, for example, sulfur vacancies on $CuIn_5S_8$ layers change the reaction pathway promoting the hydrogenation of CO* intermediates to produce CHO*, leading to high selectivity to CH_4 instead of CO molecules (Figure 14c).[147] Recently, Long and collaborators showed that the construction of twining defects on Au NPs supported on TiO_2 could improve the selectivity toward CO than regular Au-TiO_2 and bare TiO_2 materials.[151]

Another important approach to improve CO_2 activation is surface modification with organic molecules, functional groups, or cocatalysts. For example, the introduction of bismuth nanoparticles (Bi NPs) on α-Ga_2O_3 significantly improves the selectivity of CO_2 to CO (10% for bare α-Ga_2O_3 vs 80% for Bi-α-Ga_2O_3) by avoiding H_2 evolution, due to the intrinsic weak adsorption of H* species of Bi NPs, and increasing the energy barrier of the CH_2* intermediate, related to CH_4 evolution.[152] Moreover, ruthenium complexes immobilized on carbon nitride structures boost the photoreduction of CO_2 to formic acid with an impressive turnover number (>1000) and apparent quant yield (5.7%) using visible light (400 nm) and TEOA as sacrificial agent.[153] Later, Maeda et al. revealed that binuclear Ru(II) complexes supported on a system consisting of Ag/C_3N_4 significantly enhance HCOOH production with an even higher turnover number (>33 000) and elevate selectivity.[154]

Another notable approach for enhancing CO_2 activation and consequent reduction involves the stabilization of single atoms (SAs),[155] which can significantly enhance metal utilization and selectivity to a desirable product. Copper SAs supported on crystalline carbon nitrides have proven to be effective in achieving nearly 100% selectivity in carbon monoxide production.[156] The authors have elucidated that selectivity control is achieved by low-

 © 2023 The Authors. Global Challenges published by Wiley-VCH GmbH

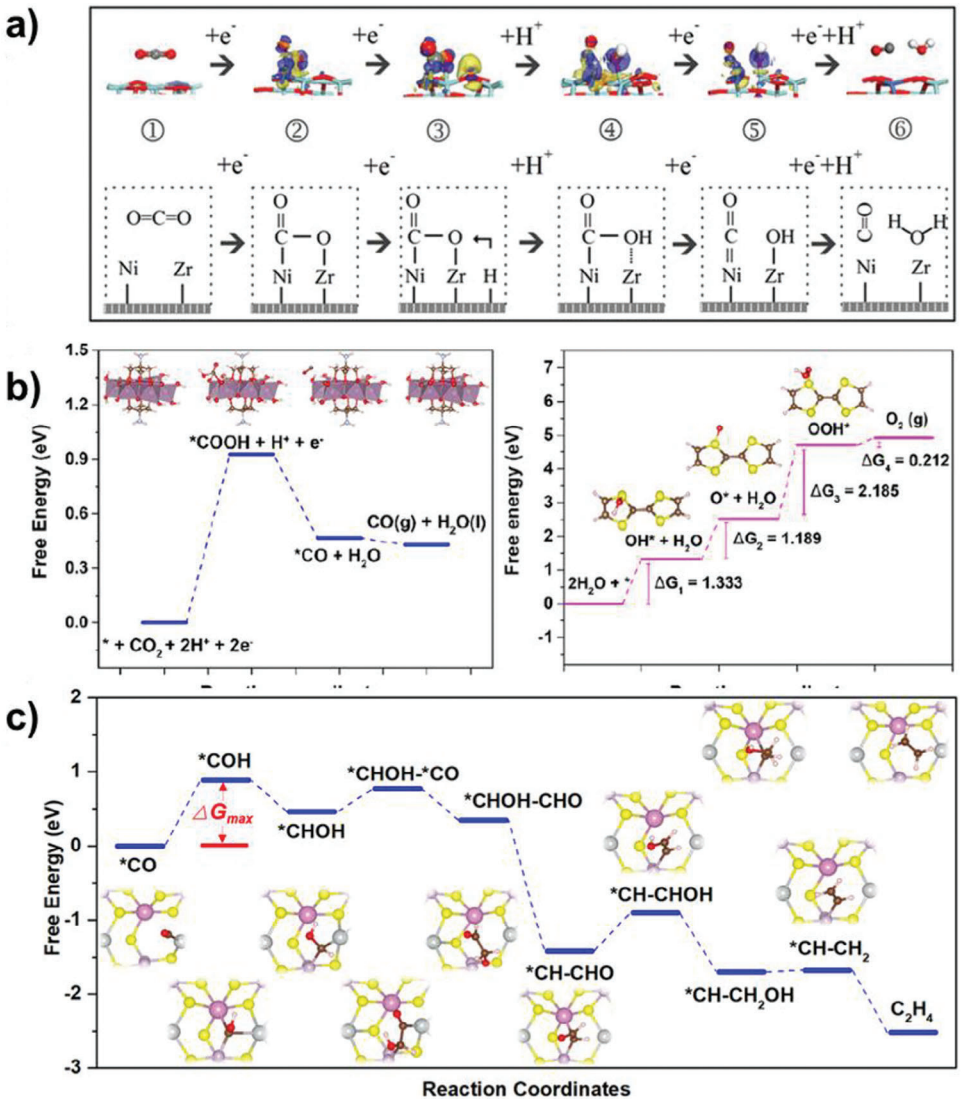


Figure 15. a) Differential charge density diagrams and intermediates during CO_2 reduction to CO over Ni-SA/O model. Reproduced with permission.[159] Copyright 2020, John Wiley and Sons; b) Free energy diagrams for CO_2 reduction to CO on $MnMo_6$ and for H_2O oxidation to O_2 on TTF of TCOF-$MnMo_6$. Reproduced with permission.[167] Copyright 2022, American Chemical Society; c) Gibbs free energy diagrams for CO reduction to C_2H_4 over $AgInP_2S_6$ with sulfur vacancies. Reproduced with permission.[174] Copyright 2021, Springer Nature.

ering the energy barrier of the deoxygenation pathway through the presence of isolated copper sites, resulting in the predominant formation of CO as the product. Moreover, the combination of single atoms (SAs) with photocatalytic systems improves CO_2 activation. For instance, Ye et al. reported that Co single atoms supported on metal-organic frameworks not only enhance charge separation through electron migration to the metal center but also reduce the energy barrier for the deoxygenation of CO_2* to CO*.[157] In addition, SAs can synergistically interact with the support material to enhance CO_2 photoreduction. The synergistic effect of Ni single atoms and the covalent organic framework (COF) structure to enhance CO production was demonstrated by Zou et al.[158] The authors suggested that the keto units present in the COF structure contribute to stabilizing COOH* intermediates, which can undergo further dehydration to generate CO. Additionally, single atoms can serve as activation centers in conjunction with atoms on the support material, leveraging their distinct catalytic abilities to function in unique ways. For instance, Ni SAs supported on defect-rich ZrO_2 promote the stabilization of COOH* species (**Figure 15**a), which can be protonated to produce CO molecules.[159] The combination of different metal activation centers has garnered interest within the research community. Furthermore, dual-single-atom materials have emerged as intriguing catalysts, as the metallic centers collaborate to enhance photocatalytic CO_2 reduction. Xiang et al. demonstrated that Co and Ru dual-single-atoms can synergistically improve charge transfer and facilitate CO_2 reduction to both CO and CH_4.[160] This dual-metallic system is able to separate charges with the assistance of Co sites while Ru centers promote CO_2 chemisorption.

 © 2023 The Authors. Global Challenges published by Wiley-VCH GmbH

5.2. CO_2 Reduction and H_2O Oxidation

Achieving high product yields in photocatalytic CO_2 reduction without the need for sacrificial agents or additives is a significant challenge. As mentioned previously, the reduction of CO_2 molecules to $CO_2^{\bullet-}$ faces considerable difficulty due to its high potential. The introduction of sacrificial agents such as TEOA, MeOH, or Na_2S can promote carbon dioxide reduction by providing protons and electrons to the system, thereby enhancing charge separation in the semiconductor. However, the use of such agents often leads to increased costs and reduced reliability. Additionally, the low solubility of carbon dioxide in water necessitates the exploration of reactions in organic media or the inclusion of basic additives to improve dissolution.

In this context, it becomes crucial to design catalysts that can efficiently reduce CO_2 molecules using only water as a sacrificial agent. For this purpose, photocatalysts must possess excellent charge separation capabilities, enabling efficient migration toward CO_2* molecules, along with appropriate band potentials that allow not only the oxidation of H_2O but also the reduction of CO_2 molecules, while preventing hydrogen evolution. The design of heterostructures has emerged as a potential approach to integrate these desired features. For example, Wong et al. developed a Z-scheme utilizing α-Fe_2O_3 and g-C_3N_4 to enhance the selectivity of CO_2 to CO without relying on sacrificial agents.[161] The authors explained that this enhanced activity arises from a combination of improved electron-hole separation and stronger CO_2 adsorption on hematite. The effectiveness of heterostructures in enhancing CO_2-to-CO reduction was further demonstrated by Li and colleagues.[162] They revealed that the Local Surface Plasma Resonance of Au nanoparticles in the ZnO/Au/ g-C_3N_4 system accelerates electron-hole separation, resulting in high CO production without the need for additives. Additionally, it has been demonstrated that AgBr/BiOBr heterojunctions with surface oxygen vacancies, exhibiting excellent charge separation and strong redox ability, serve as outstanding photocatalysts for additive-free CO_2-to-CO reduction.[163] In addition to oxides or oxyhalides, heterostructures of MOFs have been designed through hierarchical synthesis to form core-shell MOF@MOF structures. These structures exhibit enhanced charge migration and large overpotential, enabling high selectivity for the production of HCOOH (146 μmol. $g^{-1}.h^{-1}$) without the need for sacrificial agents.[164]

Beyond utilizing H_2O as an electron donor, a major aspiration in the scientific community is to develop an ideal catalyst capable of achieving artificial photosynthesis. This entails producing O_2 from water simultaneously with the conversion of CO_2 into other molecules. The main challenge lies in reconciling the complex CO_2 activation with an appropriate band diagram capable of generating oxygen through H_2O oxidation.[165] The production of O_2 is intricate due to the involvement of multielectron mechanisms. Lan et al. reported a CO/O_2 production ratio of 2:1 using a Zn-COF photocatalyst.[166] The specific activity of this material is attributed to CO_2 interaction with metal centers and H_2O oxidation occurring at C = C and S atoms of the organic linker. In a subsequent study by the same research group, a pathway was proposed not only for CO production but also for H_2O oxidation (Figure 15b). In this case, polyoxometalate clusters were incorporated into COF, leading to an O_2 evolution mechanism involving $H_2O \rightarrow OH \rightarrow O \rightarrow *OOH \rightarrow O_2$.[167] Furthermore, the "overall" CO_2 reduction was demonstrated using $BiOBr_xCl_{1-x}$ catalysts. The authors suggested that both lattice and vacancy oxygens play a role in the mechanism, with lattice oxygen responsible for O_2 generation and vacancy oxygen involved in oxygen lattice recovery and proton donation for CO production.[168]

5.3. CO_2 Reaction Mechanisms

In recent years, there has been a growing interest in the conversion of CO_2 to higher-value C_{2+} products or C_1 oxygenates, such as methanol or formic acid, as they possess greater economic value compared to commonly produced CO and CH_4. However, achieving these higher compounds is challenging due to the complex kinetics involved. For instance, the production of CH_3OH requires the generation and transfer of 6 e^- to the CO_2 molecule.[138] Despite these challenges, significant progress has been made in this field. Li and colleagues have reported the production of methanol and ethanol using a metal-organic framework (UiO6-NH_2) supported with Cu single atoms.[169] Additionally, Yang et al. demonstrated that polythiophene-modified Bi_2WO_6 could enhance charge separation and generate methanol and ethanol through CO_2 reduction.[170] The presence of Co-N_2C single-atom sites on g-C_3N_4 has shown to be responsible for CH_3OH production from CO_2, as they can simultaneously capture electrons and adsorb carbon dioxide molecules.[171]

Producing C_{2+} compounds from CO_2 reduction is particularly difficult due to the complexity of forming C-C bonds. The key step to producing such compounds is the stabilization of two adsorbed intermediates to favor the coupling between these two species. For instance, Mo et al. synthesized dual single sites (P and Cu) supported on carbon nitride and verified the formation of the coupled intermediate *OC-CHO, which is responsible for C_2H_6 production (616 μmol. $g^{-1}.h^{-1}$).[172] Zhou et al. showed that Cu single atoms on $Ti_{0.91}O_2$ atomically thin single layers can produce hydrocarbons, such as propane. The authors explained that Cu-Ti-V_O (oxygen vacancies) can stabilize *CHOCO and *CH_2OCOCO intermediates, facilitating the pathway for C-C coupling.[173] Furthermore, sulfur defects on the atomic layer of $AgInP_2S_6$ play a crucial role in accumulating charge on Ag sites and enhancing the adsorption of *CO molecules.[174] This lowers the energy barrier for C-C product formation, including ethene (Figure 15c). These findings highlight the significant advancements in the production of higher-value oxygenates and C_{2+} compounds from CO_2 reduction, despite the intricate nature of the reactions involved. Despite the intrinsic challenge of activating the CO_2 molecule, its reduction via the direct use of green H_2 in a solar-to-chemical approach is certainly the technology that holds the greatest potential among all the reactions discussed here. If successful, it can enable a path to decarbonization, leading to liquid fuels with no CO_2 footprint, besides CO_2 capture allowing in the best-case scenario a route to revert global warming.

6. Conclusions, Challenges, and Perspectives

In summary, green hydrogen has significant potential as an energy carrier and key intermediate molecule for driving the chemical industry toward a more carbon-neutral future. To achieve this

 © 2023 The Authors. Global Challenges published by Wiley-VCH GmbH

goal, it is crucial to decouple the production of valuable chemicals from hydrogen derived from fossil fuels, which has a substantial carbon footprint. Creating a sustainable, decarbonized, and environmentally friendly chemical industry demands the exploration of viable alternatives. This perspective examines traditional fossil-based processes and compares them to the potential of lab-scale photocatalytic processes as a potential substitute for hydrogen derived from fossil fuels.

Currently, photocatalytic green hydrogen production faces challenges in competitiveness compared to electrolysis powered by renewable energy sources. However, a transformative shift occurs when we customize photocatalytic systems. These systems can be finely adjusted to utilize sunlight and renewable proton sources, leading to a direct solar-to-chemical approach. In recent examples, NH_3, H_2O_2, CO_2-derived products, and chemicals produced through reduction reactions illustrate the potential of photocatalysis for creating valuable chemicals. While photocatalytic processes are not yet as efficient as commercial ones, advances in various related fields and interdisciplinary collaboration offer promising prospects for future improvements.

Today's technical challenges primarily revolve around the activity, engineering, and economic viability of photocatalysts. We believe that strategic adjustments to their structure-activity relationships can further enhance photocatalysts. Recent strategies have shown significant improvements in photocatalyst efficiency, including: 1) defect/interface engineering, 2) cocatalyst integration, 3) heterojunctions, 4) atomic doping, and 5) active site modulation, among others. These approaches hold significant promise for increasing the efficiency of solar-to-chemical processes driven by photocatalysts. Given these challenges, we assert that solar-to-chemical processes are crucial for the chemical industry's transition to a low-carbon economy.

Scaling up photoreactors to technological readiness levels 4- is also an important challenge that hinders the improvement of photocatalyst efficiency and broader acceptance in the field. Surprisingly, there is a lack of dedicated efforts focused on careful planning, simulation, and construction of pilot devices, and to a lesser extent, larger-scale plants. However, it is clear that for making industrial-scale photoreactors a reality, substantial research efforts in scaling up are essential. These efforts should aim to optimize factors such as photon utilization, mass transfer, heat management, and radiative profiles to ensure a reliable path toward large-scale implementation.

Also, the search for renewable proton sources for solar to chemical synthesis is crucial in terms of process feasibility and circular economy. The use of diverse biomass waste materials, such as microplastics, crop residues, paper, and food or organic waste, is a very appealing solution for both utilizing protons and reducing environmental pollution. Moreover, it aligns with the circular economy by effectively closing the resource loop, especially when CO_2 reduction reactions are involved.

All in all, the solar-to-chemical approach via photocatalysis offers a compelling route for collectively decarbonizing the chemical industry. In this context, strategic catalyst design and advancements in laboratory systems and photocatalytic devices will pave the way for establishing a sustainable and carbon-neutral chemical industry. Therefore, the hydrogen economy is relevant in shaping the future of the energy landscape. It contributes to sustainability, facilitates the shift away from fossil fuels, reduces carbon emissions, and improves energy security. Nevertheless, realizing its complete potential requires us to prioritize addressing cost, infrastructure, and technological challenges.

Acknowledgements

This work was financially supported by the Brazilian funding agencies CAPES, CNPq (423196/2018, 403064/2021 and 405752/2022) and FAPESP (2020/14741, 2021/13271, 2022/16273, 2021/12394, 2022/14652, 2021/13915 and 2021/11162) and the Max Planck Society. P.J.-C. received funding from the European Union's Horizon Europe research and innovation program under the Marie Skłodowska-Curie Grant Agreement N°: 101068996 for his fellowship.

Conflict of Interest

The authors declare no conflict of interest.

Keywords

chemical feedstock, green hydrogen, photocatalysis, solar energy, sustainability

Received: July 25, 2023
Revised: October 24, 2023
Published online:

[1] P. I. Jiménez-Calvo, Synthesis, charactherization, performance of g-C3N4 based materials decorated with Au nanoparticles for (photo) catalytic applications. Theoretical and/or physical chemistry. Université de Strasbourg, **2019**.
[2] a) M. Grätzel, *Nature* **2001**, *414*, 338; b) P. Jiménez-Calvo, V. Caps, M. N. Ghazzal, C. Colbeau-Justin, V. Keller, *Nano Energy* **2020**, *75*, 104888.
[3] IEA, World Energy Outlook 2023, IEA, Paris, https://www.iea.org/reports/world-energy-outlook-2023 (accessed: Auguest 2023).
[4] D. G. Nocera, *Acc. Chem. Res.* **2012**, *45*, 767.
[5] A. Züttel, A. Remhof, A. Borgschulte, O. Friedrichs, *Philos. Trans. R. Soc., A* **2010**, *368*, 3329.
[6] T. M. L. Wigley, *Climatic Change* **2018**, *147*, 31.
[7] IEA (2021), Net Zero by 2050, IEA, Paris, https://www.iea.org/reports/net-zero-by-2050. (accessed: June 2023).
[8] C. Bataille, H. Waisman, Y. Briand, J. Svensson, A. Vogt-Schilb, M. Jaramillo, R. Delgado, R. Arguello, L. Clarke, T. Wild, F. Lallana, G. Bravo, G. Nadal, G. Le Treut, G. Godinez, J. Quiros-Tortos, E. Pereira, M. Howells, D. Buira, J. Tovilla, J. Farbes, J. Ryan, D. De La Torre Ugarte, M. Collado, F. Requejo, X. Gomez, R. Soria, D. Villamar, P. Rochedo, M. Imperio, *Energy Strat. Rev.* **2020**, *30*, 100510.
[9] I. F. Teixeira, P. Jiménez-Calvo, in *Renewable Energy Production and Distribution*, Vol. *2* (Eds: M. Jeguirim, P. Dutournié), Academic Press, USA **2023**, pp. 145–180.
[10] M. Isaacs, J. Garcia-Navarro, W.-J. Ong, P. Jiménez-Calvo, *Global Challenges* **2023**, *7*, 2200165.
[11] A. L. Energies, https://usa.airliquide.com/sustainability/hydrogen/h2-storage-power#9896 (accessed: Auguest 2023).
[12] IEA (2023), World Energy Outlook 2023, IEA, Paris, https://www.iea.org/reports/world-energy-outlook-2023 (accessed: June 2023).

 © 2023 The Authors. Global Challenges published by Wiley-VCH GmbH

[13] IEA (2021), Net Zero by 2050 A Roadmap for the Global Energy Sector, IEA, Paris, https://iea.blob.core.windows.net/assets/deebef5d-0c34-4539-9d0c-10b13d840027/NetZeroby2050-ARoadmapfortheGlobalEnergySector_CORR.pdf (accessed: June 2023).
[14] IRENA (2020), Green Hydrogen: A guide to policy making, International Renewable Energy Agency, Abu Dhabi, https://www.irena.org/-/media/Files/IRENA/Agency/Publication/2020/Nov/IRENA_Green_hydrogen_policy_2020.pdf?rev=c0cf115d8c724e4381343cc93e03e9e0 (accessed: August 2023).
[15] R. W. Howarth, M. Z. Jacobson, *Energy Science & Engineering* **2021**, *9*, 1676.
[16] J. Diab, L. Fulcheri, V. Hessel, V. Rohani, M. Frenklach, *Int. J. Hydrogen Energy* **2022**, *47*, 258318.
[17] J. Garcia-Navarro, M. A. Isaacs, M. Favaro, D. Ren, W.-J. Ong, M. Grätzel, P. Jiménez-Calvo, *Global Challenges* **2023**, 2300073.
[18] a) K. C. Christoforidis, P. Fornasiero, *ChemCatChem* **2017**, *9*, 1523; b) I. F. Teixeira, J. Quiroz, M. S. Homsi, P. H. C. Camargo, *J. Braz. Chem. Soc.* **2020**, *31*, 2; c) I. F. Teixeira, N. V. Tarakina, I. F. Silva, N. Lopez-Salas, A. Savateev, M. Antonietti, *Adv. Sustainable Syst.* **2022**, *6*, 2100429; d) I. F. Teixeira, N. V. Tarakina, I. F. Silva, G. A. Atta Diab, N. L. Salas, A. Savateev, M. Antonietti, *J. Mater. Chem. A* **2022**, *10*, 181561.
[19] a) P. Jiménez-Calvo, V. Caps, V. Keller, *Renewable Sustainable Energy Rev.* **2021**, *149*, 111095; b) K. Takanabe, *ACS Catal.* **2017**, *7*, 8006.
[20] W. Liu, H. Zuo, J. Wang, Q. Xue, B. Ren, F. Yang, *Int. J. Hydrogen Energy* **2021**, *46*, 105489.
[21] IEA (2022), Global Hydrogen Review 2022, IEA, Paris, https://www.iea.org/reports/global-hydrogen-review-2022 (accessed: June 2023).
[22] IEA (2021), Ammonia Technology Roadmap, IEA, Paris, https://www.iea.org/reports/ammonia-technology-roadmap (accessed: June 2023).
[23] TechSci Research, **2023**, p. 115.
[24] B. Saha, S. De, S. Dutta, *Crit. Rev. Environ. Sci. Technol.* **2013**, *43*, 84.
[25] A. Mary, N. Kanagathara, A. R. Baby Suganthi, **2020**, *33*, 4751.
[26] G. Gao, Y. Tian, X. Gong, Z. Pan, K. Yang, B. Zong, *Chin. J. Catal.* **2020**, *41*, 1039.
[27] R. Ciriminna, L. Albanese, F. Meneguzzo, M. Pagliaro, *ChemSusChem* **2016**, *9*, 3374.
[28] P. Nikolaidis, A. Poullikkas, *Renewable Sustainable Energy Rev.* **2017**, *67*, 597.
[29] CHP (2021), Fuel Cell and Hydrogen Observatory (FCHO), CHP, https://www.clean-hydrogen.europa.eu/media/news/2021-fuel-cell-and-hydrogen-observatory-fcho-reports-2022-06-07_en (accessed: June 2023).
[30] TRC (2019), Sustainable synthetic carbon based fuels for transport, TRC, https://royalsociety.org/-/media/policy/projects/synthetic-fuels/synthetic-fuels-briefing.pdf (accessed: June 2023).
[31] a) S. Chatterjee, R. K. Parsapur, K.-W. Huang, *ACS Energy Lett.* **2021**, *6*, 4390; b) I. F. Silva, I. F. Teixeira, W. P. Barros, C. B. Pinheiro, J. D. Ardisson, G. M. do Nascimento, N. A. Pradie, A. P. C. Teixeira, H. O. Stumpf, *J. Mater. Chem. A* **2019**, *7*, 152252.
[32] M. Capdevila-Cortada, *Nat. Catal.* **2019**, *2*, 10555.
[33] J. W. Erisman, M. A. Sutton, J. Galloway, Z. Klimont, W. Winiwarter, *Nat. Geosci.* **2008**, *1*, 636.
[34] H. Ali, M. Masar, A. C. Guler, M. Urbanek, M. Machovsky, I. Kuritka, *Nanoscale Advances* **2021**, *3*, 6358.
[35] C. Smith, A. K. Hill, L. Torrente-Murciano, *Energy Environ. Sci.* **2020**, *13*, 331.
[36] S. Chen, D. Liu, T. Peng, *Sol. RRL* **2021**, *5*, 2000487.
[37] S. Mansingh, K. K. Das, S. Sultana, K. Parida, *J. Photochem. Photobiol., C* **2021**, *47*, 100402.
[38] C. J. M. van der Ham, M. T. M. Koper, D. G. H. Hetterscheid, *Chem. Soc. Rev.* **2014**, *43*, 5183.
[39] X. Chen, N. Li, Z. Kong, W.-J. Ong, X. Zhao, *Mater. Horiz.* **2018**, *5*, 9.
[40] G. N. Schrauzer, T. D. Guth, *J. Am. Chem. Soc.* **1977**, *99*, 7189.
[41] G. N. Schrauzer, N. Strampach, L. N. Hui, M. R. Palmer, J. Salehi, *Proc. Natl. Acad. Sci. USA* **1983**, *80*, 3873.
[42] J. Lee, L.-L. Tan, S.-P. Chai, *Nanoscale* **2021**, *13*, 7011.
[43] J. Li, H. Li, G. Zhan, L. Zhang, *Acc. Chem. Res.* **2017**, *50*, 112.
[44] M. Cheng, C. Xiao, Y. Xie, *J. Mater. Chem. A* **2019**, *7*, 196163.
[45] A. Steephen, Preethi V, Annenewmy B, Parthasarathy R, R. Reddy P, Sairam M, S. Kumar M, *Int. J. Hydrogen Energy* **2023**.
[46] a) M. I. Alvarado-Ávila, S. De Luca, U. Edlund, F. Ye, J. Dutta, *Sustainable Energy Fuels* **2023**, *7*, 1981; b) G. Zhang, C. Ni, X. Huang, A. Welgamage, L. A. Lawton, P. K. J. Robertson, J. T. S. Irvine, *Chem. Commun.* **2016**, *52*, 1673.
[47] J. Soria, J. C. Conesa, V. Augugliaro, L. Palmisano, M. Schiavello, A. Sclafani, *J. Phys. Chem.* **1991**, *95*, 274.
[48] T. Zhang, S. Lu, *Chem Catalysis* **2022**, *2*, 1502.
[49] Z. H. N. Al-Azri, W.-T. Chen, A. Chan, V. Jovic, T. Ina, H. Idriss, G. I. N. Waterhouse, *J. Catal.* **2015**, *329*, 355.
[50] R. Shi, Y. Zhao, G. I. N. Waterhouse, S. Zhang, T. Zhang, *ACS Catal.* **2019**, *9*, 9739.
[51] Z. Ding, M. Sun, W. Liu, W. Sun, X. Meng, Y. Zheng, *Sep. Purif. Technol.* **2021**, *276*, 119287.
[52] C. Li, M. Gu, M. Gao, K. Liu, X. Zhao, N. Cao, J. Feng, Y. Ren, T. Wei, M. Zhang, *J. Colloid Interface Sci.* **2022**, *609*, 341.
[53] Z. Zhao, S. Hong, C. Yan, C. Choi, Y. Jung, Y. Liu, S. Liu, X. Li, J. Qiu, Z. Sun, *Chem. Commun.* **2019**, *55*, 7171.
[54] a) Z. Wang, X. Hu, Z. Liu, G. Zou, G. Wang, K. Zhang, *ACS Catal.* **2019**, *9*, 102608; b) S. F. Blaskievicz, I. Freitas Teixeira, L. H. Mascaro, J. Ferreira de Brito, *ChemCatChem* **2023**, *15*, 202201610.
[55] G. F. S. R. Rocha, M. A. R. da Silva, A. Rogolino, G. A. A. Diab, L. F. G. Noleto, M. Antonietti, I. F. Teixeira, *Chem. Soc. Rev.* **2023**, *52*, 4878.
[56] Y. Sun, Y. Ahmadi, K.-H. Kim, J. Lee, *Renewable Sustainable Energy Rev.* **2022**, *170*, 112967.
[57] T. T. Hou, H. L. Peng, Y. Xin, S. M. Wang, W. K. Zhu, L. L. Chen, Y. Yao, W. H. Zhang, S. Q. Liang, L. B. Wang, *ACS Catal.* **2020**, *10*, 5502.
[58] L. Li, Y. Yu, S. Lin, W. Chu, D. Sun, Q. Su, S. Ma, G. Du, B. Xu, *Catal. Commun.* **2021**, *153*, 106294.
[59] a) L. Fan, Q. Yu, J. Chen, U. Khan, X. Wang, J. Gao, *Catalysts* **2022**, *12*, 9; b) W. Gao, X. Li, X. Zhang, S. Su, S. Luo, R. Huang, Y. Jing, M. Luo, *Nanoscale* **2021**, *13*, 7801.
[60] H. Li, J. Shang, Z. Ai, L. Zhang, *J. Am. Chem. Soc.* **2015**, *137*, 6393.
[61] P. Li, Z. Zhou, Q. Wang, M. Guo, S. Chen, J. Low, R. Long, W. Liu, P. Ding, Y. Wu, Y. Xiong, *J. Am. Chem. Soc.* **2020**, *142*, 124309.
[62] Y. Chen, S. Ji, C. Chen, Q. Peng, D. Wang, Y. Li, *Joule* **2018**, *2*, 1242.
[63] S. P. Zhang, B. Bai, J. Liu, J. T. Zhang, *Catalysts* **2021**, 11.
[64] Q. S. Wang, D. F. Zhang, Y. Chen, W. F. Fu, X. J. Lv, *ACS Sustainable Chem. Eng.* **2019**, *7*, 6430.
[65] P. C. Huang, W. Liu, Z. H. He, C. Xiao, T. Yao, Y. M. Zou, C. M. Wang, Z. M. Qi, W. Tong, B. C. Pan, S. Q. Wei, Y. Xie, *Sci. China-Chem.* **2018**, *61*, 1187.
[66] S. Wu, Z. Chen, W. Yue, S. Mine, T. Toyao, M. Matsuoka, X. Xi, L. Wang, J. Zhang, *ACS Catal.* **2021**, *11*, 4362.
[67] a) Q. Liu, J. Yuan, Z. Gan, C. Liu, J. Li, Y. Liang, R. Chen, *ACS Sustainable Chem. Eng.* **2021**, *9*, 560; b) Y. Zhao, R. Shi, X. Bian, C. Zhou, Y. Zhao, S. Zhang, F. Wu, G. I. N. Waterhouse, L.-Z. Wu, C.-H. Tung, T. Zhang, *Adv. Sci.* **2019**, *6*, 1802109; c) P.-W. Huang, M. C. Hatzell, *Nat. Commun.* **2022**, *13*, 7908.
[68] R. E. Brooks, S. B. Moore, *Cellulose* **2000**, *7*, 263.
[69] a) M. G. C. Baldry, *J. Appl. Bacteriol.* **1983**, *54*, 417; b) W. H. Glaze, J.-W. Kang, D. H. Chapin, *Ozone: Sci. Eng.* **1987**, *9*, 335.
[70] L. Plant, M. Jeff, *Chemical Engin.* **1994**, *101*, 16.

 © 2023 The Authors. Global Challenges published by Wiley-VCH GmbH

[71] a) C. C. Winterbourn, *Toxicol. Lett.* **1995**, *82*, 969; b) J. J. Pignatello, E. Oliveros, A. MacKay, *Crit. Rev. Environ. Sci. Technol.* **2006**, *36*, 1.
[72] a) S. Fukuzumi, Y. Yamada, K. D. Karlin, *Electrochim. Acta* **2012**, *82*, 493; b) L. An, T. Zhao, X. Yan, X. Zhou, P. Tan, *Sci. Bull.* **2015**, *60*, 55.
[73] MaM (2022), Market Research Report, Hydrogen Peroxide Market by Grade (90% H_2O_2, 35% H_2O_2, 6 TO 10% H_2O_2, 3% H_2O_2), Application, End-use Industry (Pulp & Paper, Food & Beverage, Water Treatment, Textiles & Laundry, Oil & Gas, Healthcare, Electronics), & Region - Global Forecast to 2027, MaM (accessed: July 2023).
[74] J. K. Edward, S. J. Freakley, R. J. Lewis, J. C. Pritchard, G. J. Hutchings, *Catal. Today* **2015**, *248*, 3.
[75] X. Wang, C. K. Law, *J. Chem. Phys.* **2013**, *138*, 134305.
[76] J. M. Campos-Martin, G. Blanco-Brieva, J. L. G. Fierro, *Angew. Chem., Int. Ed.* **2006**, *45*, 6962.
[77] T. Nishimi, T. Kamachi, K. Kato, T. Kato, K. Yoshizawa, *Eur. J. Org. Chem.* **2011**, *2011*, 4113.
[78] Y. Sun, L. Han, P. Strasser, *Chem. Soc. Rev.* **2020**, *49*, 6605.
[79] H. Hou, X. Zeng, X. Zhang, *Angew. Chem., Int. Ed.* **2020**, *59*, 173566.
[80] Z. Chen, D. Yao, C. Chu, S. Mao, *Chem. Eng. J.* **2023**, *451*, 138489.
[81] Y. Shiraishi, S. Kanazawa, Y. Sugano, D. Tsukamoto, H. Sakamoto, S. Ichikawa, T. Hirai, *ACS Catal.* **2014**, *4*, 774.
[82] H. J. Baumgartner, G. C. Hood, J. M. Monger, R. M. Roberts, C. E. Sanborn, *J. Catal.* **1963**, *2*, 405.
[83] Y. Wang, Y. Wang, J. Zhao, M. Chen, X. Huang, Y. Xu, *Appl. Catal., B* **2021**, *284*, 119691.
[84] A. Moncayo-Lasso, C. Pulgarin, N. Benítez, *Water Res.* **2008**, *42*, 4125.
[85] W. Xing, M. Yin, Q. Lv, Y. Hu, C. Liu, J. Zhang, in *Rotating Electrode Methods and Oxygen Reduction Electrocatalysts* (Eds: W. Xing, G. Yin, J. Zhang), Elsevier, Amsterdam, **2014**, pp. 1–31.
[86] Y. Zhao, P. Zhang, Z. Yang, L. Li, J. Gao, S. Chen, T. Xie, C. Diao, S. Xi, B. Xiao, C. Hu, W. Choi, *Nat. Commun.* **2021**, *12*, 3701.
[87] D. Banerjee, N. Kushwaha, N. P. Shetti, T. M. Aminabhavi, E. Ahmad, *Renewable Sustainable Energy Rev.* **2022**, *167*, 112827.
[88] J. Liu, Y. Zou, B. Jin, K. Zhang, J. H. Park, *ACS Energy Lett.* **2019**, *4*, 3018.
[89] D. K. Chauhan, S. Jain, V. R. Battula, K. Kailasam, *Carbon* **2019**, *152*, 40.
[90] S. Zhao, T. Guo, X. Li, T. Xu, B. Yang, X. Zhao, *Appl. Catal., B* **2018**, *224*, 725.
[91] S. Zhao, X. Zhao, H. Zhang, J. Li, Y. Zhu, *Nano Energy* **2017**, *35*, 405.
[92] A. Malathi, J. Madhavan, M. Ashokkumar, P. Arunachalam, *Appl. Catal., A* **2018**, *555*, 47.
[93] H. Hirakawa, S. Shiota, Y. Shiraishi, H. Sakamoto, S. Ichikawa, T. Hirai, *ACS Catal.* **2016**, *6*, 4976.
[94] S. Xu, Y. Kim, D. Higgins, M. Yusuf, T. F. Jaramillo, F. B. Prinz, *Electrochim. Acta* **2017**, *255*, 99.
[95] A. Rogolino, I. F. Silva, N. V. Tarakina, M. A. R. da Silva, G. F. S. R. Rocha, M. Antonietti, I. F. Teixeira, *ACS Appl. Mater. Interfaces* **2022**, *14*, 498209.
[96] Y. Isaka, Y. Kawase, Y. Kuwahara, K. Mori, H. Yamashita, *Angew. Chem., Int. Ed.* **2019**, *58*, 5402.
[97] L. Chen, S. Li, Z. Yang, C. Chen, C. Chu, B. Chen, *Appl. Catal., B* **2022**, *305*, 121066.
[98] L. Li, L. Xu, Z. Hu, J. C. Yu, *Adv. Funct. Mater.* **2021**, *31*, 2106120.
[99] U. Nwosu, A. Wang, B. Palma, H. Zhao, M. A. Khan, M. Kibria, J. Hu, *Renewable Sustainable Energy Rev.* **2021**, *148*, 111266.
[100] T. Uekert, H. Kasap, E. Reisner, *J. Am. Chem. Soc.* **2019**, *141*, 152010.
[101] J. Zhang, P. Yu, G. Zeng, F. Bao, Y. Yuan, H. Huang, *J. Mater. Chem. A* **2021**, *9*, 9685.
[102] J. Zhang, L. Zheng, F. Wang, C. Chen, H. Wu, S. A. K. Leghari, M. Long, *Appl. Catal., B* **2020**, *269*, 118770.
[103] Z. Teng, Q. Zhang, H. Yang, K. Kato, W. Yang, Y.-R. Lu, S. Liu, C. Wang, A. Yamakata, C. Su, B. Liu, T. Ohno, *Nat. Catal.* **2021**, *4*, 374.
[104] L. Fan, X. Bai, C. Xia, X. Zhang, X. Zhao, Y. Xia, Z.-Y. Wu, Y. Lu, Y. Liu, H. Wang, *Nat. Commun.* **2022**, *13*, 2668.
[105] C. Chu, Q. Zhu, Z. Pan, S. Gupta, D. Huang, Y. Du, S. Weon, Y. Wu, C. Muhich, E. Stavitski, K. Domen, J.-H. Kim, *Proc. Natl. Acad. Sci. USA* **2020**, *117*, 6376.
[106] Y. Shiraishi, S. Kanazawa, D. Tsukamoto, A. Shiro, Y. Sugano, T. Hirai, *ACS Catal.* **2013**, *3*, 2222.
[107] Y. Kofuji, Y. Isobe, Y. Shiraishi, H. Sakamoto, S. Ichikawa, S. Tanaka, T. Hirai, *ChemCatChem* **2018**, *10*, 2070.
[108] L. Zhang, M. Zhou, A. Wang, T. Zhang, *Chem. Rev.* **2020**, *120*, 683.
[109] D. Wang, D. Astruc, *Chem. Rev.* **2015**, *115*, 6621.
[110] M. Guo, M. Zhang, R. Liu, X. Zhang, G. Li, *Adv. Sci.* **2022**, *9*, 2103361.
[111] a) M. A. Garcia, *J. Phys. D: Appl. Phys.* **2011**, *44*, 283001; b) Z. Liu, Y. Huang, Q. Xiao, H. Zhu, *Green Chem.* **2016**, *18*, 817.
[112] X. Zhang, X. Li, M. E. Reish, D. Zhang, N. Q. Su, Y. Gutiérrez, F. Moreno, W. Yang, H. O. Everitt, J. Liu, *Nano Lett.* **2018**, *18*, 1714.
[113] J. Song, Z.-F. Huang, L. Pan, K. Li, X. Zhang, L. Wang, J.-J. Zou, *Appl. Catal., B* **2018**, *227*, 386.
[114] T. Jia, D. Meng, H. Ji, H. Sheng, C. Chen, W. Song, J. Zhao, *Appl. Catal., B* **2022**, *304*, 121004.
[115] K. Su, Y. Wang, C. Zhang, Z. Gao, J. Han, F. Wang, *Appl. Catal., B* **2021**, *298*, 120554.
[116] C. Deng, S. Xie, Y. Li, Y. Zhao, P. Zhou, H. Sheng, H. Ji, C. Chen, J. Zhao, *The Journal of Physical Chemistry A* **2023**, *127*, 2787.
[117] R. Nie, Y. Tao, Y. Nie, T. Lu, J. Wang, Y. Zhang, X. Lu, C. C. Xu, *ACS Catal.* **2021**, *11*, 1071.
[118] K. Tsutsumi, F. Uchikawa, K. Sakai, K. Tabata, *ACS Catal.* **2016**, *6*, 4394.
[119] Y. Huang, Z. Liu, G. Gao, Q. Xiao, W. Martens, A. Du, S. Sarina, C. Guo, H. Zhu, *Catal. Sci. Technol.* **2018**, *8*, 726.
[120] a) X. Zhang, J. Chen, Y. Gao, K. Li, Y. Zhou, W. Sun, B. Fan, *Org. Chem. Front.* **2019**, *6*, 2410; b) E. Zhao, W. Zhang, L. Dong, R. Zbořil, Z. Chen, *ACS Catal.* **2023**, *13*, 7557.
[121] F. Arcudi, L. Đorđević, N. Schweitzer, S. I. Stupp, E. A. Weiss, *Nat. Chem.* **2022**, *14*, 1007.
[122] Y. Guo, J. Chen, *RSC Adv.* **2016**, *6*, 101968.
[123] a) Z. Yu, Z. Chen, Y. Chen, Q. Peng, R. Lin, Y. Wang, R. Shen, X. Cao, Z. Zhuang, Y. Li, *Nano Res.* **2018**, *11*, 3730; b) M. Li, N. Zhang, R. Long, W. Ye, C. Wang, Y. Xiong, *Small* **2017**, *13*, 1604173; c) C. Han, L. Du, M. Konarova, D.-C. Qi, D. L. Phillips, J. Xu, *ACS Catal.* **2020**, *10*, 9227.
[124] E. Zhao, M. Li, B. Xu, X.-L. Wang, Y. Jing, D. Ma, S. Mitchell, J. Pérez-Ramírez, Z. Chen, *Angew. Chem., Int. Ed.* **2022**, *61*, e202207410.
[125] T. Jia, D. Meng, R. Duan, H. Ji, H. Sheng, C. Chen, J. Li, W. Song, J. Zhao, *Angew. Chem., Int. Ed.* **2023**, *62*, e202216511.
[126] B. Zhou, J. Song, H. Zhou, T. Wu, B. Han, *Chem. Sci.* **2016**, *7*, 463.
[127] F. Xu, K. Meng, S. Cao, C. Jiang, T. Chen, J. Xu, J. Yu, *ACS Catal.* **2022**, *12*, 164.
[128] F. Yao, L. Dai, J. Bi, W. Xue, J. Deng, C. Fang, L. Zhang, H. Zhao, W. Zhang, P. Xiong, Y. Fu, J. Sun, J. Zhu, *Chem. Eng. J.* **2022**, *444*, 136430.
[129] T. Pirali, M. Serafini, S. Cargnin, A. A. Genazzani, *J. Med. Chem.* **2019**, *62*, 5276.
[130] a) Y. Kostyukevich, T. Acter, A. Zherebker, A. Ahmed, S. Kim, E. Nikolaev, *Mass Spectrometry Reviews* **2018**, *37*, 811; b) M. Miyashita, M. Sasaki, I. Hattori, M. Sakai, K. Tanino, *Science* **2004**, *305*, 495.
[131] a) A. Katsnelson, *Nat. Med.* **2013**, *19*, 656; b) M. M. Midland, S. Greer, A. Tramontano, S. A. Zderic, *J. Am. Chem. Soc.* **1979**, *101*, 2352; c) B. Belleau, J. Burba, M. Pindell, J. Reiffenstein, *Science* **1961**, *133*, 102.
[132] X. Ling, Y. Xu, S. Wu, M. Liu, P. Yang, C. Qiu, G. Zhang, H. Zhou, C. Su, *Sci. China: Chem.* **2020**, *63*, 386.

 © 2023 The Authors. Global Challenges published by Wiley-VCH GmbH

[133] C. Liu, Z. Chen, C. Su, X. Zhao, Q. Gao, G.-H. Ning, H. Zhu, W. Tang, K. Leng, W. Fu, B. Tian, X. Peng, J. Li, Q.-H. Xu, W. Zhou, K. P. Loh, *Nat. Commun.* **2018**, *9*, 80.
[134] Y. Guo, W. An, X. Tian, L. Xie, Y.-L. Ren, *Green Chem.* **2022**, *24*, 9211.
[135] C. Han, G. Han, S. Yao, L. Yuan, X. Liu, Z. Cao, A. Mannodi-Kanakkithodi, Y. Sun, *Adv. Sci.* **2022**, *9*, 2103408.
[136] X.-L. Nan, Y. Wang, X.-B. Li, C.-H. Tung, L.-Z. Wu, *Chem. Commun.* **2021**, *57*, 6768.
[137] a) S. Chu, Y. Cui, N. Liu, *Nat. Mater.* **2017**, *16*, 16; b) D. E. H. J. Gernaat, H. S. de Boer, V. Daioglou, S. G. Yalew, C. Müller, D. P. van Vuuren, *Nat. Clim. Change* **2021**, *11*, 119.
[138] J. Albero, Y. Peng, H. García, *ACS Catal.* **2020**, *10*, 5734.
[139] a) L. Ding, T. Shi, J. Gu, Y. Cui, Z. Zhang, C. Yang, T. Chen, M. Lin, P. Wang, N. Xue, L. Peng, X. Guo, Y. Zhu, Z. Chen, W. Ding, *Chem* **2020**, *6*, 2673; b) J. S. Derrick, M. Loipersberger, R. Chatterjee, D. A. Iovan, P. T. Smith, K. Chakarawet, J. Yano, J. R. Long, M. Head-Gordon, C. J. Chang, *J. Am. Chem. Soc.* **2020**, *142*, 20489; c) K. Jiang, R. B. Sandberg, A. J. Akey, X. Liu, D. C. Bell, J. K. Nørskov, K. Chan, H. Wang, *Nat. Catal.* **2018**, *1*, 111.
[140] G. Chen, G. I. N. Waterhouse, R. Shi, J. Zhao, Z. Li, L.-Z. Wu, C.-H. Tung, T. Zhang, *Angew. Chem., Int. Ed.* **2019**, *58*, 17528.
[141] U. Ulmer, T. Dingle, P. N. Duchesne, R. H. Morris, A. Tavasoli, T. Wood, G. A. Ozin, *Nat. Commun.* **2019**, *10*, 3169.
[142] E. Gong, S. Ali, C. B. Hiragond, H. S. Kim, N. S. Powar, D. Kim, H. Kim, S.-I. In, *Energy Environ. Sci.* **2022**, *15*, 880.
[143] J. Wu, Y. Huang, W. Ye, Y. Li, *Adv. Sci.* **2017**, *4*, 1700194.
[144] X. Chang, T. Wang, J. Gong, *Energy Environ. Sci.* **2016**, *9*, 2177.
[145] a) H. J. Freund, M. W. Roberts, *Surf. Sci. Rep.* **1996**, *25*, 225; b) H. J. Freund, R. P. Messmer, *Surf. Sci.* **1986**, *172*, 1.
[146] T. Kong, Y. Jiang, Y. Xiong, *Chem. Soc. Rev.* **2020**, *49*, 6579.
[147] X. Li, Y. Sun, J. Xu, Y. Shao, J. Wu, X. Xu, Y. Pan, H. Ju, J. Zhu, Y. Xie, *Nat. Energy* **2019**, *4*, 690.
[148] Y. Ji, Y. Luo, *J. Am. Chem. Soc.* **2016**, *138*, 15896.
[149] Y. Pu, Y. Luo, X. Wei, J. Sun, L. Li, W. Zou, L. Dong, *Appl. Catal., B* **2019**, *254*, 580.
[150] J. Wu, X. Li, W. Shi, P. Ling, Y. Sun, X. Jiao, S. Gao, L. Liang, J. Xu, W. Yan, *Angew. Chem.* **2018**, *130*, 8855.
[151] H. Huang, J. Zhao, B. Weng, F. Lai, M. Zhang, J. Hofkens, M. B. Roeffaers, J. A. Steele, J. Long, *Angew. Chem., Int. Ed.* **2022**, *61*, e202204563.
[152] P. Chen, K. Li, L. Chen, W. Zhang, Y. Zhou, F. Dong, Y. Sun, *ACS Sustainable Chem. Eng.* **2023**, *11*, 7182.
[153] R. Kuriki, K. Sekizawa, O. Ishitani, K. Maeda, *Angew. Chem., Int. Ed.* **2015**, *54*, 2406.
[154] R. Kuriki, H. Matsunaga, T. Nakashima, K. Wada, A. Yamakata, O. Ishitani, K. Maeda, *J. Am. Chem. Soc.* **2016**, *138*, 5159.
[155] L. Ran, Z. Li, B. Ran, J. Cao, Y. Zhao, T. Shao, Y. Song, M. K. H. Leung, L. Sun, J. Hou, *J. Am. Chem. Soc.* **2022**, *144*, 17097.
[156] Y. Li, B. Li, D. Zhang, L. Cheng, Q. Xiang, *ACS Nano* **2020**, *14*, 10552.
[157] H. Zhang, J. Wei, J. Dong, G. Liu, L. Shi, P. An, G. Zhao, J. Kong, X. Wang, X. Meng, *Angew. Chem.* **2016**, *128*, 14522.
[158] W. Zhong, R. Sa, L. Li, Y. He, L. Li, J. Bi, Z. Zhuang, Y. Yu, Z. Zou, *J. Am. Chem. Soc.* **2019**, *141*, 7615.
[159] X. Xiong, C. Mao, Z. Yang, Q. Zhang, G. I. Waterhouse, L. Gu, T. Zhang, *Adv. Energy Mater.* **2020**, *10*, 2002928.
[160] L. Cheng, X. Yue, L. Wang, D. Zhang, P. Zhang, J. Fan, Q. Xiang, *Adv. Mater.* **2021**, *33*, 2105135.
[161] Z. Jiang, W. Wan, H. Li, S. Yuan, H. Zhao, P. K. Wong, *Adv. Mater.* **2018**, *30*, 1706108.
[162] X. Li, H. Jiang, C. Ma, Z. Zhu, X. Song, H. Wang, P. Huo, X. Li, *Appl. Catal., B* **2021**, *283*, 119638.
[163] Z. Miao, Q. Wang, Y. Zhang, L. Meng, X. Wang, *Appl. Catal., B* **2022**, *301*, 120802.
[164] H. B. Huang, Z. B. Fang, R. Wang, L. Li, M. Khanpour, T. F. Liu, R. Cao, *Small* **2022**, *18*, 2200407.
[165] M. Jerigova, Y. Markushyna, I. F. Teixeira, B. Badamdorj, M. Isaacs, D. Cruz, I. Lauermann, M. Á. Muñoz-Márquez, N. V. Tarakina, N. López-Salas, O. Savateev, P. Jimenéz-Calvo, *Adv. Sci.* **2023**, *10*, 2300099.
[166] M. Lu, J. Liu, Q. Li, M. Zhang, M. Liu, J. L. Wang, D. Q. Yuan, Y. Q. Lan, *Angew. Chem.* **2019**, *131*, 12522.
[167] M. Lu, M. Zhang, J. Liu, T.-Y. Yu, J.-N. Chang, L.-J. Shang, S.-L. Li, Y.-Q. Lan, *J. Am. Chem. Soc.* **2022**, *144*, 1861.
[168] M. Gao, J. Yang, T. Sun, Z. Zhang, D. Zhang, H. Huang, H. Lin, Y. Fang, X. Wang, *Appl. Catal., B* **2019**, *243*, 734.
[169] G. Wang, C.-T. He, R. Huang, J. Mao, D. Wang, Y. Li, *J. Am. Chem. Soc.* **2020**, *142*, 19339.
[170] W. Dai, H. Xu, J. Yu, X. Hu, X. Luo, X. Tu, L. Yang, *Appl. Surf. Sci.* **2015**, *356*, 173.
[171] M. Ma, Z. Huang, D. E. Doronkin, W. Fa, Z. Rao, Y. Zou, R. Wang, Y. Zhong, Y. Cao, R. Zhang, Y. Zhou, *Appl. Catal., B* **2022**, *300*, 120695.
[172] G. Wang, Z. Chen, T. Wang, D. Wang, J. Mao, *Angew. Chem., Int. Ed.* **2022**, *61*, e202210789.
[173] Y. Shen, C. Ren, L. Zheng, X. Xu, R. Long, W. Zhang, Y. Yang, Y. Zhang, Y. Yao, H. Chi, J. Wang, Q. Shen, Y. Xiong, Z. Zou, Y. Zhou, *Nat. Commun.* **2023**, *14*, 1117.
[174] W. Gao, S. Li, H. He, X. Li, Z. Cheng, Y. Yang, J. Wang, Q. Shen, X. Wang, Y. Xiong, Y. Zhou, Z. Zou, *Nat. Commun.* **2021**, *12*, 4747.



Gabriel Ali Atta Diab has BSc degree in chemistry from the University of Brasília (2021). Currently, he is a PhD candidate at Federal University of São Carlos (UFSCar), supervised by Prof. Ivo Freitas Teixeira. His research field is focused on investigating heterogeneous photocatalysts applied to energy production, particularly in hydrogen evolution, natural gas photo-oxidation, CO_2 reduction, as well as other applications in organic molecule synthesis.

 © 2023 The Authors. Global Challenges published by Wiley-VCH GmbH



Marcos A. R. da Silva received his master's degree in Inorganic Chemistry at the Federal University of São Carlos (UFSCar), Brazil in 2021. Currently, he is a PhD student at the UFSCar and a researcher fellow at Brazilian Agricultural Research Corporation (Embrapa). His research focuses on the development of metal single-atoms coordinated at crystalline carbon nitrides for oxidation reactions, especially selective oxidation of C—H bonds, such as methane photooxidation.



Guilherme F. S. R. Rocha obtained his BSc in Chemistry from University of São Paulo (USP) in 2021 currently his is undegoing his master's degree under the supervision of Prof. Ivo at the University of Sao Carlos (UFSCar) and it is expected to finish by 2024. His research interests include synthesis of heterogeneous catalysts with a focus with photocatalytic applications for chemical synthesis and energy conversion.



Luis Fernando Guimarães Noleto majored in Chemistry at Universidade Estadual e Federal do Piauí (UESPI/UFPI, Brazil), where he investigated the photocatalytic properties of silver phosphate (Ag_3PO_4). He is currently studying for a doctorate with Prof. Ivo F. Teixeira, focusing on the development of catalysts based on crystalline carbon nitride and single-atoms, applied in photocatalytic production of hydrogen peroxide and ammonia, as well as in the selective hydrogenation of organic compounds.



Andrea Rogolino received his BSc (2020) and MSc (2022) in Chemistry from the University of Padova, Italy, where he was a fellow student at the Galilean School of Higher Education. In 2021, he was a visiting student at the Max Planck Institute of Colloids and Interfaces in Potsdam, Germany. He is currently a PhD candidate in the Reisner Lab at the University of Cambridge. He nurtures a strong passion for every field of Chemistry since his participation in the International Chemistry Olympiads in 2016 and 2017. His actual research interests are photo(electro)chemical devices for solar fuel production.

 © 2023 The Authors. Global Challenges published by Wiley-VCH GmbH



João Paulo de Mesquita received his PhD in Inorganic Chemistry from the University of Minas Gerais (UFMG, 2012). He carried out two postdoctoral research at the UFMG (2013), and the Federal University of São Carlos (UFSCAR, 2023). He is currently an Associate Professor at the Federal University of Vales Jequitinhonha and Mucuri where he coordinates the research group on Technologies in Hybrid, Porous and Polymeric Materials. During the last 10 years he has supervised several master and PhD candidates, published articles related to different materials and applications. His research is mainly associated with Chemistry of Interfaces of graphene based materials and g-C_3N_4 for different applications.



Pablo Jiménez Calvo is an MSCA Post-doctoral fellow and lecturer at Friedrich-Alexander-Universität Erlangen-Nürnberg, Germany. He received his PhD in Materials Chemistry and Physics from the University of Strasbourg in 2019, and conducted postdoctoral research at the Max Planck Institute of Colloids and Interfaces (Prof. Antonietti, 2022), and the University of Paris-Saclay (Dr. Paineau, 2020). He develops energy interfaces for solar-driven photoelectrocatalysis: carbon nitrides, heterojunctions, and metals. He published 15 articles, 1 book chapter, and 37 presentations. He was finalist for the Rising Star of Materials Today Catalysis (2023) and the European Young Chemist's award of the EuChemS (2020).



Ivo F. Teixeira received his BS in 2012 and his MSc in 2013 from the Federal University of Minas Gerais. He received his PhD from the University of Oxford in 2017. Between 2020 and 2022, Ivo was a Humboldt Fellow at the Max Planck Institute of Colloids and Interfaces (Potsdam, Germany). He became Assistant Professor at the Federal University of São Carlos (Brazil) in 2019, since then Ivo and 12 students under his supervision have fun every day doing science. His research group is focused on catalysis, especially heterogeneous catalysis, single-atom catalysis, energy conversion and nanomaterials.

 © 2023 The Authors. Global Challenges published by Wiley-VCH GmbH